GEND-INF- 023
Vol. IV
March 1983

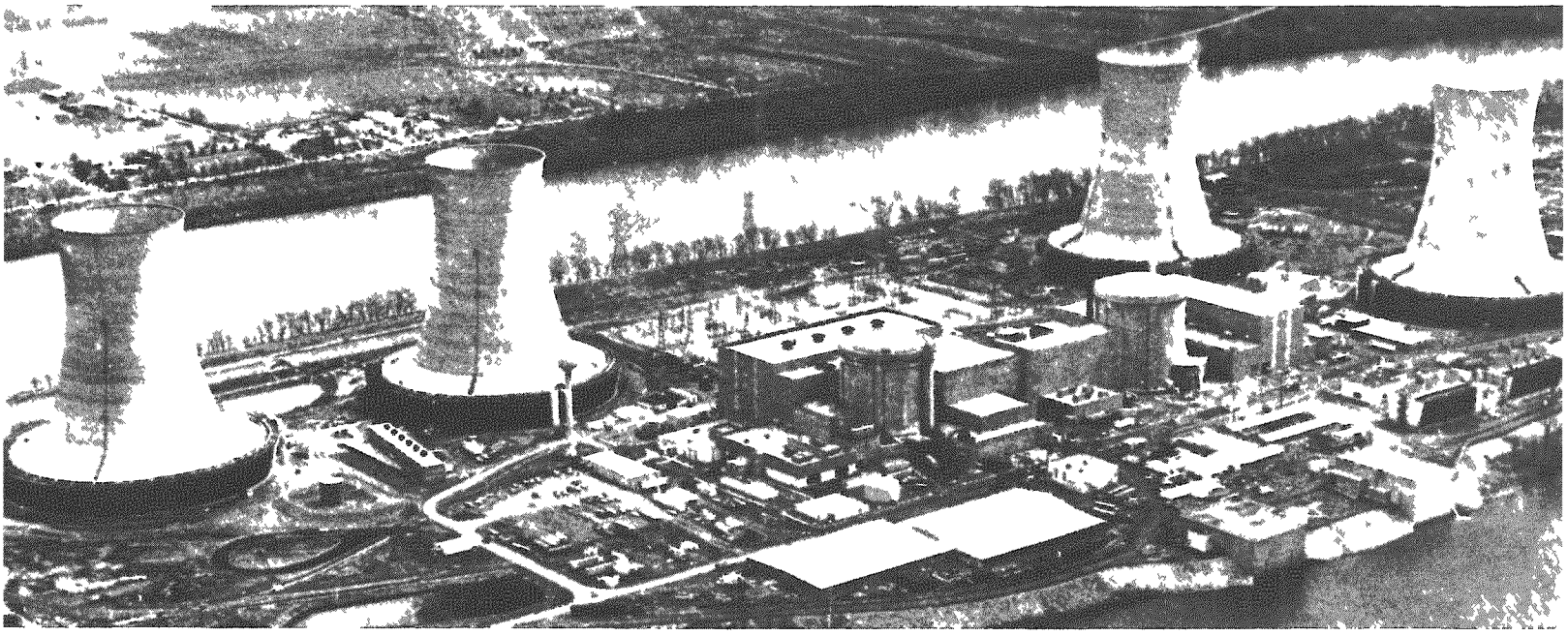

This is an informal report intended for use as a preliminary or working document

GEND

General Public Utilities • Electric Power Research Institute • U.S. Nuclear Regulatory Commission • U.S. Department of Energy

ANALYSIS OF THE THREE MILE ISLAND UNIT 2 HYDROGEN BURN

J.O. Henrie
A.K. Postma

Prepared for the
U.S. Department of Energy
Three Mile Island Operations Office
Under DOE Contract No. DE-AC07-76ID01570

DISCLAIMER

DISCLAIMER

GEND-INF--023-Vol.4

DE83 012186

GEND-INF-023
Volume IV

ANALYSIS OF THE THREE MILE ISLAND UNIT 2 HYDROGEN BURN

J.O. Henrie
A.K. Postma

Published March 1983

Rockwell International
Rockwell Hanford Operations
Richland, Washington 99352

DISCLAIMER

Prepared for EG&G Idaho, Inc.
and the U.S. Department of Energy
Three Mile Island Operations Office
Under DOE Contract No. DE-AC07-76ID01570

ABSTRACT

As a basis for the analysis of the hydrogen burn which occurred in the Three Mile Island Containment on March 28, 1979, a study of recorded temperatures and pressures was made. Long-term temperature information was obtained from the multipoint temperature recorder which shows 12 containment atmosphere temperatures plotted every 6 min. The containment atmosphere pressure recorder provided excellent long- and short-term pressure information. Short-term information was obtained from the multiplex record of 24 channels of data, recorded every 3 sec, and the alarm printer record which shows status change events and prints out temperatures, pressures, and the time of the events. The timing of these four data recording systems was correlated and pertinent data were tabulated, analyzed, and plotted to show average containment temperature and pressure versus time. Photographs and videotapes of the containment entries provided qualitative burn information.

Hydrogen concentrations were calculated using the following information:

a. Analysis of the burn peak projected back to a theoretical zero-time burn

b. Gas addition from containment temperature and pressure measurements before the hydrogen burn

c. Gas depletion from containment temperature and pressure measurements before and after the hydrogen burn

d. Rate of pressure rise during the burn

e. Oxygen depletion from chemical analyses.

Postburn average ambient temperatures versus time were calculated from recorded pressure data, and from empirical data obtained from shock tube tests conducted by Rockwell in 1973.[1] Average temperatures were calculated for the region above elevation 347, below elevation 347, and within the D-ring compartments.

The analyses indicate the following:

1. Prior to the burn, the hydrogen was well mixed with the containment air. The average hydrogen concentration was calculated to be 7.9%, wet basis.

2. The hydrogen burn occurred at all three levels in the containment. The burn was initiated somewhere in the lowest level; probably on the west side. Even though the burn time was about 15 sec, nearly all of the burning occurred during a 6-sec period. Over one-half of the burning occurred during the last 3-sec period.

3. About 3,570 standard (0°C) cubic meters (126,000 standard cubic feet), 160 kg (351 lb) moles or 319 kg of hydrogen burned. Approximately 1.1% hydrogen remained after the burn and 0.6% was released from the reactor cooling system to containment during the first hour after the burn.

4. Containment gas temperatures in the flame front were about 760°C (1400°F). The average containment gas temperature at the end of the burn was about 660°C (1220°F).

5. The gas temperatures decreased much faster below elevation 347 (large ratio of exposed surface area to containment gas volume) than above elevation 347 (low ratio of exposed surface area to containment gas volume). Curves are presented which show the calculated average gas temperatures versus time in these two containment zones and in the D-rings.

6. The average temperature rise of all materials and components in the reactor building, including the containment shell, was calculated to be only about 1.2°C (2.2°F) as a result of the hydrogen burn. Considerably more energy came from the hot water and steam vented from the cooling system to the containment than from the hydrogen burn. This resulted in the massive shield temperatures increasing an average of about 4°C (8°F) in 2 days. In the long-term, most of the heat was removed by the air coolers.

The burn damage observed was predominantly at the upper elevations and on the east and south quadrants. The vertical distribution resulted not only from the lower ratio of exposed surface area to gas volume at the upper elevations, but also from a more complete burning at the higher elevations. Therefore, significant damage to hydrocarbon materials would be expected at high elevations and not at low elevations.

The reason for lack of burn damage on the west side is probably due to the steam vent from the coolant drain tank terminating on that side. Temperature data show the west side temperatures heating rapidly while steam was venting, then actually subcooling (from evaporation of wet surfaces) after steam venting was terminated. Similar heating and cooling did not occur on the east side. Therefore, walls, floors, and equipment on the west side were very wet and evaporation kept their temperatures near or below the boiling point of water throughout much of the postburn cooling period.

On the north side the D-rings are relatively close to the containment wall, resulting in a large ratio of exposed surface area to containment gas volume. This condition causes rapid cooling which minimizes burn damage.

Approximately 1.1% hydrogen remained in the containment after the burn. Venting of the reactor cooling system during the hour following the burn added an additional 0.6%. Hydrogen concentrations increased

from this 1.7% to about 2.2% between March 30 and April 2 as the reactor cooling system was vented. One of two Rockwell hydrogen recombiners was operated for 1 month and removed 112 kg of hydrogen. When recombiner operation was terminated, the containment hydrogen concentration was 0.7%. This hydrogen was vented to the atmosphere in July 1980.

A total of 459 kg of hydrogen gas were accounted for. Assuming somewhat arbitrarily that 90% of the hydrogen was generated by the zirconium-steam reaction and 10% by radiolysis, 9,300 kg (20,500 lb) of zirconium would have been oxidized.

CONTENTS

FIGURES:

TABLES:

1.0 INTRODUCTION

On March 28, 1979, as a result of a very unlikely series of adverse events, the Three Mile Island-2 (TMI-2) reactor core lost coolant, overheated, and reactor core zirconium reacted with steam, oxidized, and liberated large quantities of hydrogen. Most of this hydrogen was exhausted to the reactor containment where it later ignited. This hydrogen burn has been analyzed with the following objectives:

1. To determine how much hydrogen was produced and how much burned

2. To gain an overall understanding of the nature of the burn, including the reasons for the nonuniform burn damage which was later observed.

The major reasons for the first objective are (a) to assist in projecting the extent of reactor core damage and thereby to allow better planning for the clean-up and disposal operation and (b) to provide a correct evaluation of TMI-2 conditions to be used as a basis for safety rules being developed that are consistent with the potential for core damage and hydrogen generation. A primary reason for the second objective is that a basis is needed for the design of equipment which would remain operable during and after similar burns.

The analysis was conducted based on actual recorded data obtained from the TMI data center. Empirical information and methods of calculation were obtained from existing reliable sources or developed from experience. The four major sources of TMI data and a brief description of each follow. To avoid confusion, the data are presented in the units indicated by the instrumentation, rather than converting the data to SI units.

1.1 REACTIMETER

The reactimeter which was installed at TMI-2 is owned by Babcock & Wilcox, and was used during plant startup and operation. It monitors 24 data points 5 times each second and was programmed to record the data at 3-sec intervals. This record provided the major source of short-term containment pressure information. The steam generator steam pressure monitors utilize differential pressure devices which use the containment pressure as the zero reference pressure. Therefore, as the containment pressure increased it had the effect of indicating a corresponding drop in steam pressure. Assuming little or no change in steam conditions during the burn and initial cooling period, containment pressure points were recorded each 3 sec for each steam generator. Reactimeter time was corrected to correlate with computer time by comparing definitive spike or step changes recorded on both systems. Based on the times of the turbine trip and reactor scram, 1 min and 10 or 11 sec would be added to the reactimeter time to equal computer time. At the time of peak containment pressure at the end of the hydrogen

burn, only 1 min 5.5 sec would be added to the reactimeter time to equal computer time. This indicates a shift in reactimeter/computer timing during the 9 hr 50 min period preceding the burn.

1.2 CONTAINMENT PRESSURE RECORDER

The containment pressure recorder operating at the time of the hydrogen burn has two ranges, -5 to 10 psig (67 to 170 kPa absolute) and 0 to 100 psig (101 to 786 kPa absolute). Therefore, a good continuous record of containment pressure is available from this recorder and was used extensively in the analysis. With care, the time can be read to less than 1 min. A few spot checks indicate that about 30 sec should be subtracted from the indicated recorder time to equal computer time.

1.3 PLANT COMPUTER

The plant computer sets the time for the entire plant and other timing systems are corrected to it for comparisons. Unless otherwise indicated, times stated in this report are computer time.

1.3.1 Alarm Printer

The alarm printer indicates the time when any of a large number of computer monitored events occur. The printer indicates "low," "high," or "norm" (returned to normal), and provides a printed record of the temperature, pressure, or flow, etc., as appropriate. When an event occurs and the reading is off scale, the printer indicates "bad" and prints question marks in the parameter column. Another indication is "cont," for "contact input." This is for open/close contact inputs and the printer indicates the resulting conditions such as high, low, trip, isolation, normal, etc. in the parameter column. Events are automatically scanned on a preplanned basis. The pressure data used herein appear to be on a 1-sec scan period. The temperature data appear to be on a 30-sec scan period. The time printed for an event represents the time the scan was completed. The order in which the events are printed for a given scan is the programmed scanning order, not the chronological order. Therefore, a thermal event could have actually occurred up to 30 sec prior to the printed alarm time.

1.3.2 Utility Printer

The utility printer provides the operator with special summary, trend, and sequence-of-events reports. The summary and trend reports list the numerical values of selected data points at various times. The time shown for each line is the time at which printing of the line started, not the actual time associated with the printed parameter. The sequence-of-events reports accurately display the sequential timing of a series of events recorded in the computer memory.

1.4 MULTIPOINT TEMPERATURE RECORDER

This recorder prints 24 points (numbered 1 through 24) every 6 min, or one point every 15 sec. The chart speed is 4.5 in./hr. The first four points indicate primary shield temperatures. Points 5 through 16 indicate ambient air temperatures as described in Table 1-1. Points 17 to 24 are spares and print near zero.

This recorder provided the only long-term temperature information available for the containment atmosphere. Unfortunately, it was printing points 17 through 24 and 1 through 4 during the hydrogen burn and initial cooldown. Nevertheless, the data provided were very useful in the analysis. A copy of the chart was obtained and time-corrected for the first few days following the event.

TABLE 1-1. Temperature Recorder Points and Their Response to Pressurizer Relief Valve (PRV) Opening (steam dumping).

Number	Location			Response
	Angle from north	Elevation (ft)	Radius (ft)	
5	150° (in east end of air cooler duct)	319	60	Moderate
6	210° (in west end of air cooler duct)	323	60	Extensive - subcools after PRV is closed
7	170°	288	44	Little
8	10°	288	52	Little
9	355°	288	46	Little
10	225° (in coolant drain tank room)	288	41	Little - only after long delay
11	90	353	45	Little - this sensor became wet from containment spray and remained wet for about 10 hr
12	285	353	56	Extensive - subcools after PRV is closed
13	255° (near stairwell No. 1)	326	61	Most extensive - subcools extensively after PRV is closed
14	100°	330	50	Little
15	260°	310	60	Moderate - got hotter and stayed hotter longer than No. 16 (on the east side) but did not appear to subcool after PRV closed
16	135°	310	51	Moderate

2.0 PREBURN CONDITIONS

2.1 THERMAL-HYDRAULIC CONDITIONS

Prior to the hydrogen burn at 13:50, the containment atmosphere had been heated repeatedly by steam released from the reactor coolant system (RCS). Temperature measurements showed that the containment atmosphere was cooled rapidly by the containment air coolers each time the pressurizer relief valve (PRV - specifically block valve RC-V2) was closed. At 13:49 on March 28, 1979, the PRV had been closed for approximately 42 min, except for one brief period starting at 13:21. At that time one of three temperature sensors on piping in that area alarmed high. An analysis of typical alarm and reset times for these three sensors and an analysis of containment temperature trends indicate that the PRV was open for only a very short period and that the amount of heat or water vapor entering the containment was insignificant. By 13:49 the containment coolers had reduced the gas temperature at sensing point 12, located at elevation 353 ft, to 53°C (128°F). Due to its high elevation and apparent protection from the containment spray, this temperature sensing point is believed to indicate temperatures nearer the average for the entire containment than any other temperature sensing point. Interestingly, this temperature is the same as the temperature indicated at 04:00 just prior to reactor trip. Key conditions of the containment atmosphere just prior to the burn are summarized in Table 2-1.

TABLE 2-1. Thermal-Hydraulic Conditions at the Containment Building Just Prior to the Hydrogen Burn at 13:50.

Parameter	State or value
Average gas temperature	53.3°C (128°F)
Gas pressure	110.3 kPa (16.0 psia)
Estimated water vapor concentration	3.5 vol%
Air cooler flow rate	110.9 m^3/sec (235,000 ACFM)
PRV	Had been open for 1/2 to 1 min

The data presented in Table 2-1 were determined by a study of recorder charts and an analysis of the performance of the air coolers. Air cooler flow rate is based on all five coolers operating (recently concluded by Burns and Roe and TMI-2 personnel).

2.2 HYDROGEN INVENTORY

A study of temperatures and pressures in the RCS indicate that hydrogen was generated at a significant rate beginning at approximately 06:14. This is indicated by a pressure increase in the RCS that occurred at that time even though the PRV was open and the apparent release of fission products prior to PRV closure at approximately 06:20. Hydrogen generation continued at a significant rate until approximately 06:54 when coolant pump RC-P-2B was operated. The flow of water into the core caused a rapid pressure rise, and also apparently terminated the metal-water reaction. This timing of hydrogen generation generally agrees with earlier analyses presented by Wooten et al.[2] and by Cole.[3]

Radiation monitors in containment began indicating increases in radioactivity at about 06:20. One example is radiation monitor HP-R-213 located in the incore instrument service area. Numerous radiation monitors indicated responses by 06:30 (4). It is likely that the monitors were detecting radioactivity which escaped from the RCS before the PRV was closed. The response time delay probably represents the time required for the radioactivity to be transported through the reactor coolant drain tank (RCDT) and its vent line, then through the air coolers and exhaust ducts to the various parts of the building where the monitors are located. The alternative is that the transfer of gas from the RCS occurred through an unidentified leak path after the PRV was closed. However, most of the hydrogen that escaped from the RCS no doubt did so during times when the PRV was open. The time-history of hydrogen mass in the containment building was reconstructed using the following data:

- Timing of projected hydrogen generation in the core
- Timing of the PRV openings
- Pressure changes in the RCS
- Calculated quantity of hydrogen consumed in the burn
- Measured quantity of hydrogen present in containment after the burn.

Results from this analysis are exhibited graphically in Figure 2-1. Perhaps the most important result shown on Figure 2-1 is that the hydrogen accumulated in the containment atmosphere over a 6 to 7 hr time period allowing mixing processes to distribute hydrogen throughout the containment volume. As indicated on Figure 2-1, essentially all of the hydrogen that was in the containment prior to the burn had been there for 1 to 7 hr, providing a relatively long mixing time. The exception to this is the small quantity of hydrogen that was released when the PRV opened just prior to the burn. Only a relatively small quantity of hydrogen would have entered containment during this period because the PRV was open for less than 1 min and because the RCS pressure was relatively low and much of the hydrogen had already been dumped at earlier times.

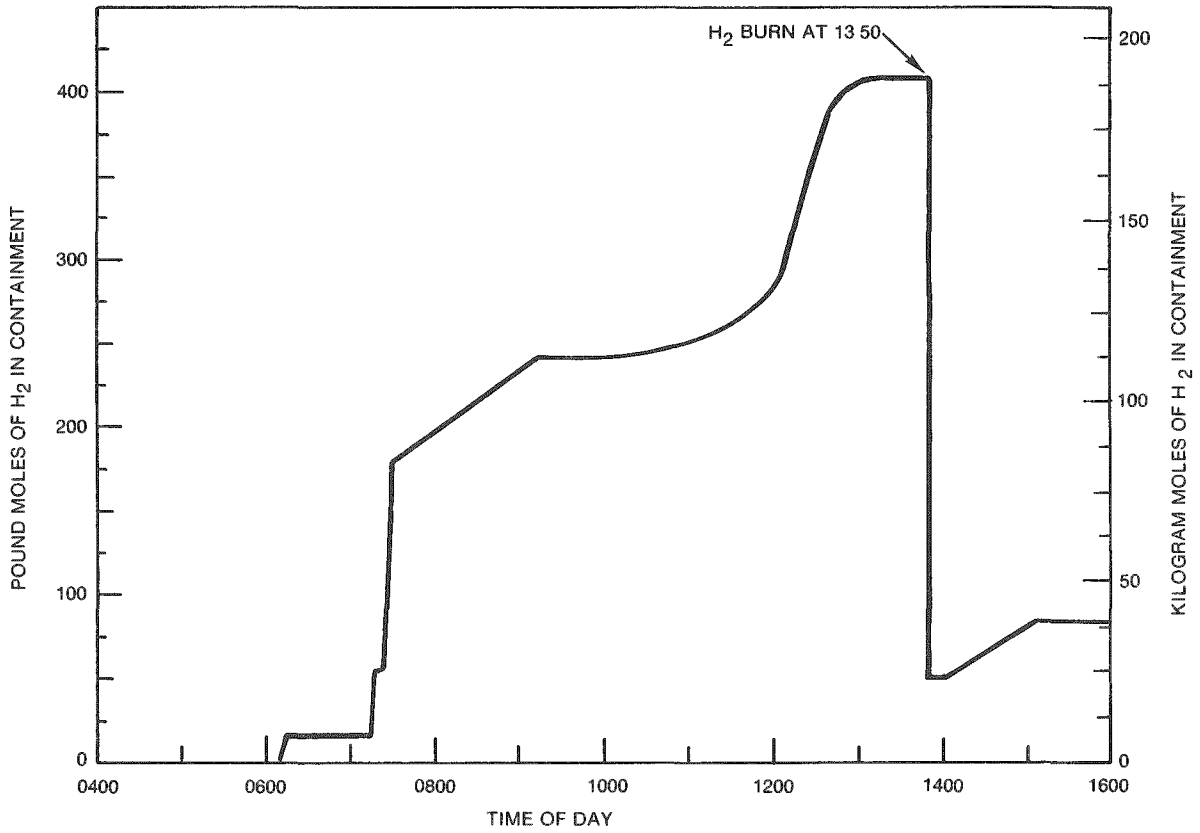

FIGURE 2-1. Projection of Hydrogen Accumulation in Containment.

2.3 HYDROGEN MIXING

The main entry point of hydrogen to the containment atmosphere was the discharge duct from the RCDT. This duct [0.46 m (18-in.)] diameter delivered gas exiting from the failed rupture disc to a point outside the room which housed the RCDT. The duct terminates below the elevation 305 (93 m) floor at a point reasonably close to the west (No. 1) stairway which is open at each floor. Temperatures measured at elevation 326 in the vicinity of this stairway (sensing point No. 13 on the multipoint recorder) reacted quickly to steam exiting from the RCDT exhaust duct, indicating that the steam plume had passed this point. The hydrogen/steam mixtures entered other containment spaces through the open stairway, floor gratings and an annular gap about 4 in. wide between each floor and the containment shell.

The hydrogen/steam mixture would be initially highly buoyant and would tend to stratify in each of the compartments into which it entered.

The tendency of hydrogen/steam mixtures to stratify is opposed by a number of mixing processes. Among these are the following:

- Entrainment by the exiting jet or plume
- Natural convection due to temperature gradients along wall surfaces
- Molecular diffusion
- Momentum of air exiting from air cooler outlet ducts
- Inter-room mixing caused by air flow from the air coolers.

Experiments conducted under the support of the Electric Power Research Institute (EPRI)[5] have illustrated the degree of mixing that occurs in a large test vessel when heated hydrogen/steam mixtures are jetted in at a local point. The test compartment was 7.6 m (25 ft) in diameter and 4.6 m (15 ft) in height, and represented a 0.3 size scale of the lower annular compartment of an ice condenser containment. It was demonstrated that appreciable hydrogen concentration gradients could persist only during the injection phase. After the source was terminated, hydrogen concentrations became uniform (to within a fraction of 1% hydrogen) within a few minutes.

In the TMI-2 containment all of the mixing mechanisms noted above were operational. Temperature differences of 10°C to 30°C (20°F to 60°F) typically existed between gas and walls, ensuring the existence of turbulent boundary layers on walls. Also, the coolers recirculated containment air an average of once every 8 to 9 min. For most of the hydrogen in containment, these mixing processes had hours to operate making it almost certain that the bulk of the hydrogen would have been well mixed throughout the containment space. The small quantity of hydrogen released during the period when the PRV was open immediately prior to the burn would, of course, not have had time to mix with all of the contained gas, and small local volumes of higher hydrogen concentration would have existed at the time the burn began.

In summary, a cursory application of existing mixing data to the TMI-2 preburn atmosphere leads to the conclusion that at the time of the burn, the bulk of the hydrogen was well mixed throughout the containment atmosphere. Except for the region of the vent plume, it is unlikely that concentration differences as much as 1% hydrogen could have existed between the upper containment and regions below elevation 305.

3.0 HYDROGEN BURN

3.1 CONTAINMENT PRESSURES AND TEMPERATURES

As previously stated, the containment pressures resulting from the hydrogen burn are shown on the pressure recorder and the steam pressure monitors for the Once Through Steam Generators (OTSG), A and B. There were also 10 pressure switches calibrated to actuate at about 24.7 kPa (3.58 psig) and to reset at about 20.7 kPa (3 psig) and 6 pressure switches calibrated to actuate at about 184 kPa (26.75 psig) and to reset at about 180 kPa (26 psig). These switches were monitored by the plant computer; therefore, the times that these switches actuated and reset are accurately known. Pressure switch actuation data are detailed in Table 3-1. Based on these accurately timed and calibrated data, the OTSG A and B pressure data were corrected by adding 1 min 5-1/2 sec to the reactimeter time for that period, adjusting the pressure at the time the hydrogen burn started to 9.0 kPa (1.3 psig) (from the pressure recorder), then increasing the indicated value of each pressure point by 7.7%, a span correction which matches the calibrated pressure points. A plot of these data near the time of the end of the burn is shown in Figure 3-1. A composite of the data available from all three sources, from the time just prior to the hydrogen burn until after the containment spray was terminated, is shown in Figure 3-2. The average containment gas/vapor temperature was calculated from the containment pressure (after the hydrogen burn) by the following expression, and the resulting temperature scale was added to Figures 3-1 and 3-2.

$$T_2 = \frac{P_2\, T_1}{P_1\left(1 - \frac{\%H_2 \text{ burned}}{200}\right)}$$

where

T_1 = initial absolute temperature

T_2 = absolute temperature at the time of interest

P_1 = initial absolute pressure

P_2 = absolute pressure at the time of interest.

This expression corrects for the hydrogen and oxygen burned and the water vapor produced by the reaction. Its accuracy assumes no condensation (or addition) of water vapor. Note that the temperature is the containment average which includes the lowest (air cooler outlet) to the highest (dome) containment gas temperatures. Of the available temperature sensors, sensing point No. 12 is believed to best represent this average temperature.

TABLE 3-1. Pressure Switch Actuation and Reset Time Data from the Alarm Printer During the Hydrogen Burn.

Rack No./ color	Penetration No./length	Elevation/ angle	Channel RB No.	Switch BSPS	Input No.	Actuate time	Norm time	Trip calibration check (psig)		Reset calibration check 07/82 (psig)	Reset corrected to 03/79 calibration (psig)
								03/79	07/82		
472/red	545A/64 ft	324 ft/ 15°	1A	3259	2833	50:21	53:37	--	3.5	3.4	
			1B	3987	3278	50:21	55:15	--	3.4	2.85	
									3.5	2.8	
			--	3570	3167	50:21.3	53:14	--	3.58	3.15	
								--	3.52	3.2	
								--	3.5	--	
			4A	3253	2836	50:27	50:32	27.05	25.5	24.1	25.8
								--	25.9	24.8	
								--	26.1	24.8	
			4B	3256	3281	50:27	50:31	27.85	28.15	27.2	26.75
								--	27.0	26.1	
								--	26.55	25.1	
455/green	554C/28 ft	319 ft/ 40°	2A	3260	2834	50:21	54:01	--	3.58	3.35	
			2B	3988	3279	50:21	54:03	--	3.6	3.3	
			--	3571	3168	50:21.0	01:44	--	3.55	3.0	
								--	3.50	3.1	
								--	3.75	2.4	
			5A	3254	2837	50:27	50:32	27.30	25.8	24.7	26.3
								--	26.1	25.3	
								--	24.9	23.8	
			5B	3257	3264	50:26	50:32	26.60	25.9	24.5	25.4
								--	25.5	24.6	
								--	26.5	25.1	
467/ yellow	562C/60 ft	319 ft/ 45°	3A	3261	2835	50:21	59.15	--	3.8	3.3	
			3B	3989	3280	50:21	53:32	--	3.55	3.40	
			--	3572	3169	50:21.2	53:49	--	3.55	3.1	
								--	3.55	3.2	
								--	3.45	3.33	
			6A	3255	2838	50:27	50:32	27.75	27.6	25.3	25.8
								--	27.4	25.9	
								--	28.2	26.1	
			6B	3258	3265	50:27	50:31	27.35	26.6	25.4	26.2
								--	26.6	25.5	
								--	26.9	25.7	
452/blue	571C/30 ft	293 ft/ 45°	--	3573	3170	50:21.4	52:53	--	--	--	

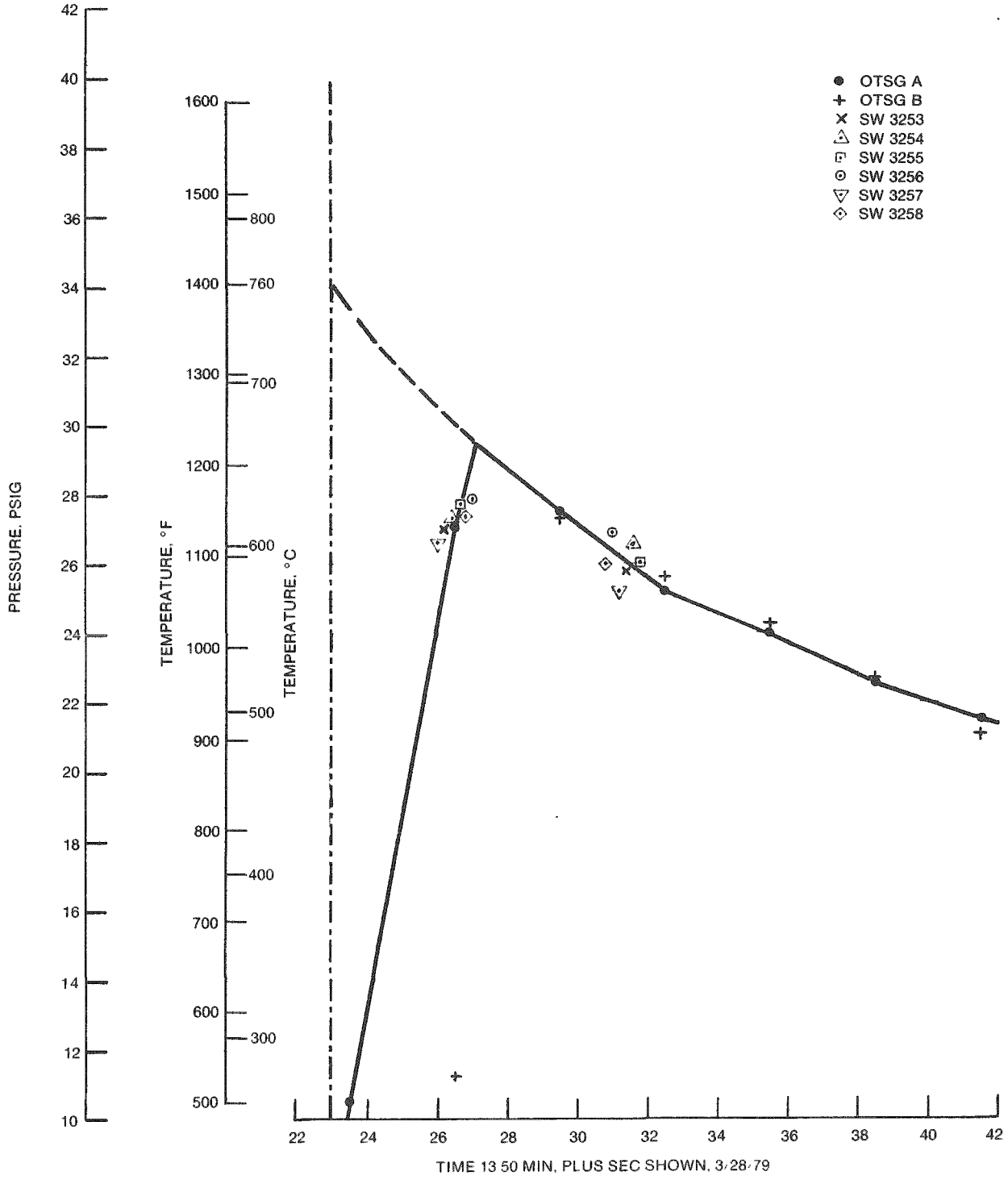

FIGURE 3-1. Peak Containment Pressure and Average Temperature Projected Back to a Theoretical "zero-time" Burn.

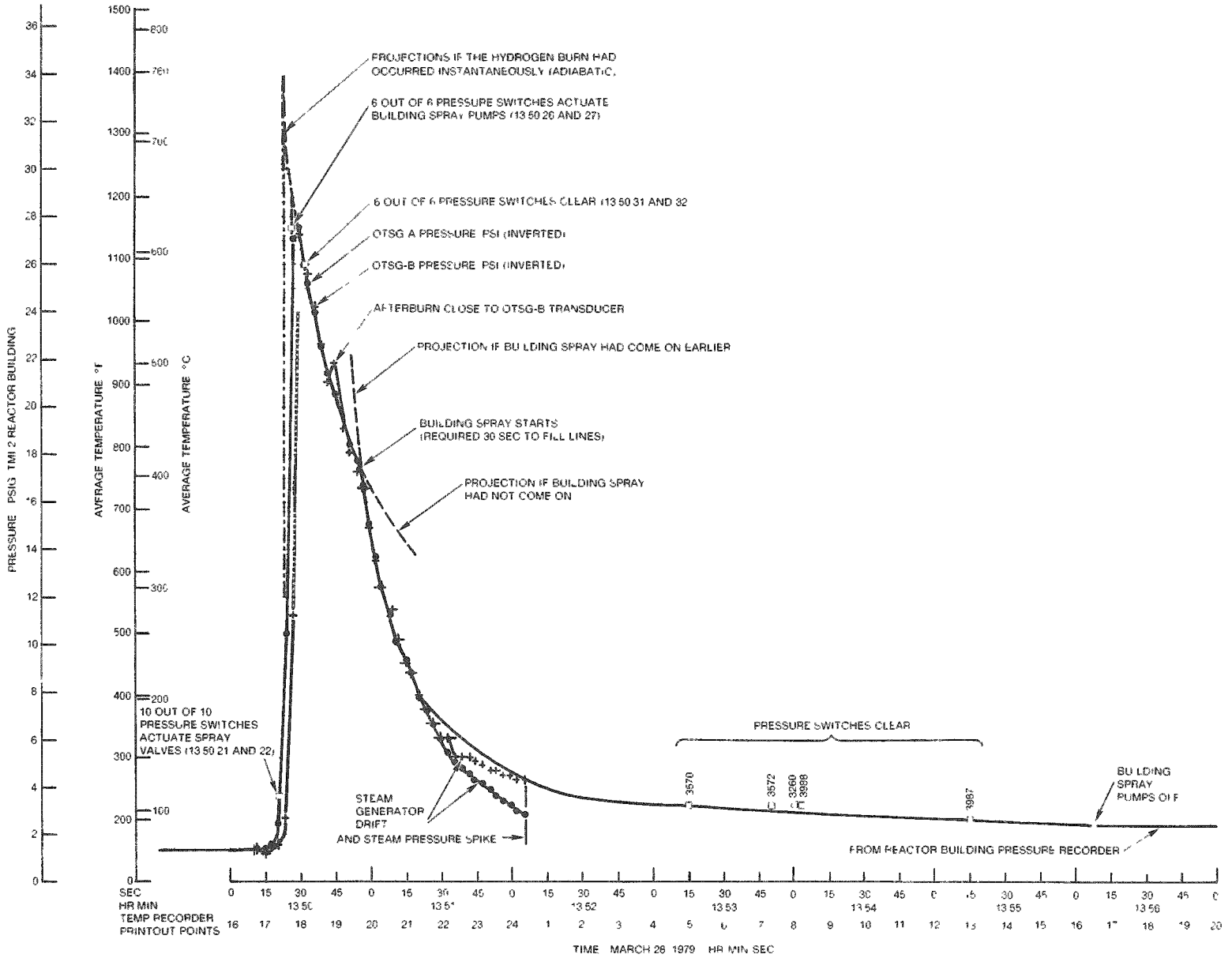

FIGURE 3-2. Composite TMI-2 Containment Average Temperature and Pressure Versus Time.

3.2 QUANTITY OF HYDROGEN BURNED

The quantity of hydrogen burned was calculated using five different methods; these methods are listed in what is believed to be the order of best accuracy:

1. Analysis of the burn peak pressure-temperature projected back in time to a theoretical "zero-time" (adiabatic) burn
2. Gas addition calculated from containment temperature and pressure measurements before the hydrogen burn
3. Gas depletion calculated from containment temperature and pressure measurements just prior to and after the hydrogen burn
4. Pressure rise rate and flame front velocities during the burn
5. Oxygen depletion from chemical analyses.

3.2.1 Theoretical "Zero-Time" Burn

The projection or extrapolation of the burn pressure-temperature back to a theoretical "zero-time" burn is shown on Figure 3-1. The time selected for the theoretical burn was based on a trial and error approximation method which balanced the integral of the temperature times the cooling time before the theoretical burn, with that after the theoretical burn to the end of the burn. This method resulted in the time for the theoretical burn to be 4 sec prior to the end of the burn as indicated by the measured peak pressure. The extrapolation based on empirical heat transfer information (to be discussed later) also appears to be consistent with a graphical projection of the measured data points. This extrapolation/projection crosses the theoretical burn time at 760°C (1400°F). This temperature should be increased by approximately 30°C (50°F) to 790°C (1450°F) to compensate for the afterburn which occurred at about 13:50:45. (See Section 4.3.) From a plot of the predicted containment temperature for an adiabatic, isochoric, hydrogen burn shown in Figure 3-3, the hydrogen burn consumed 6.8% hydrogen on a total wet (3.5% water vapor) basis.

3.2.2 Gas Addition

Gas addition calculations have suffered from the difficulty of accurately predicting the quantities of water vapor present in the containment atmosphere at different times. A study was made of the effect the gas coolers have on the water vapor content or relative humidity of the containment gas. It was found that the gas coolers are very efficient in removing water vapor from the containment. With five blowers operating at full flow, 22.2 m^3/sec (47,000 ft^3/min) each, the 57,600 m^3

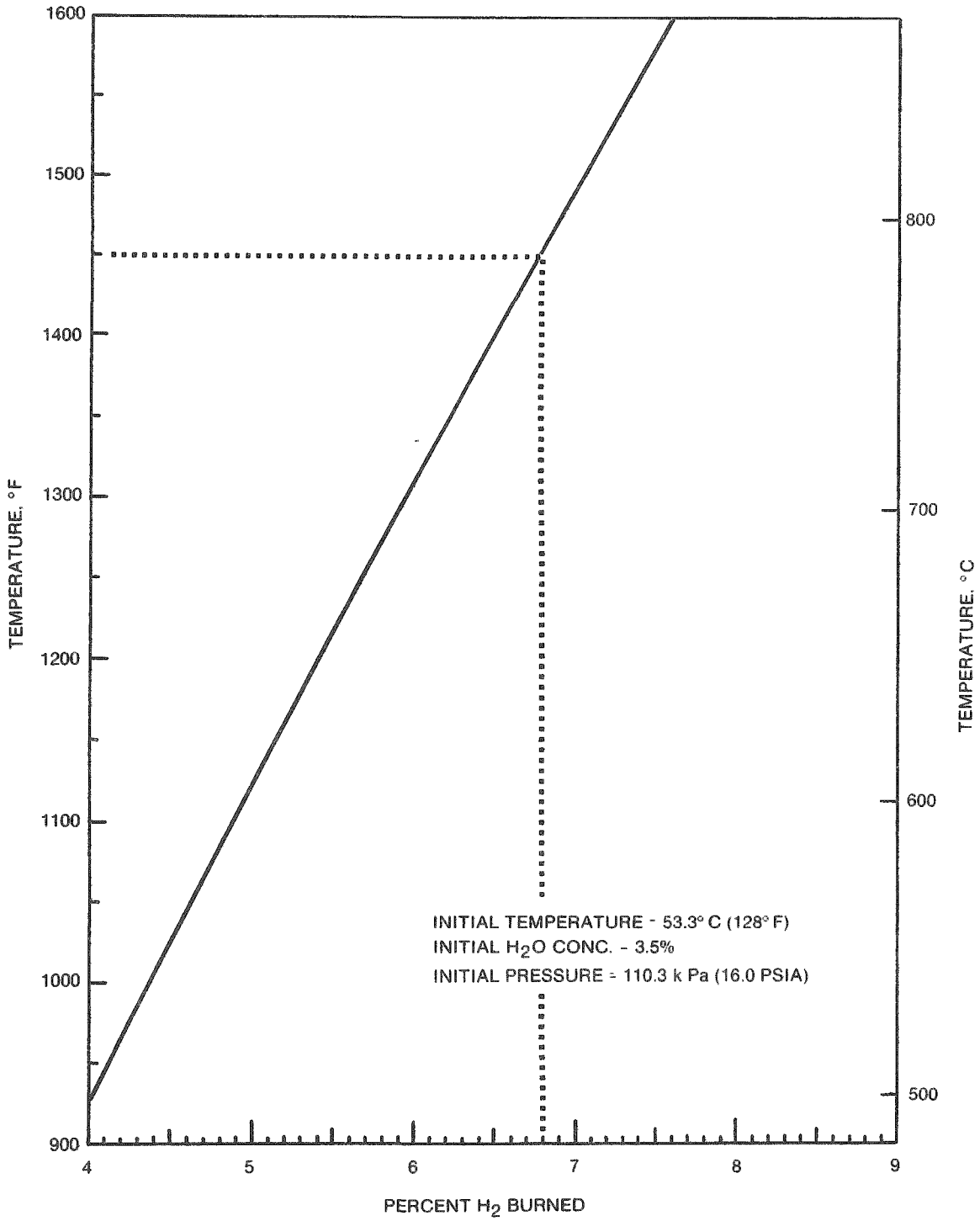

FIGURE 3-3. Predicted Containment Temperature for an Adiabatic Isochoric Hydrogen Burn.

(2,033,000 ft^3) of gas in the containment goes through the air coolers once every 8.65 min. Therefore, in 42 min the containment gas volume passes through the coolers an average of 4.85 times. With perfect mixing, and with no change in gas cooler outlet temperature, this would reduce the water vapor to within 3.5% of that of the saturated gas leaving the gas coolers. This is lower than should be expected since mixing is not perfect, and the gas cooler outlet temperature was decreasing as inlet temperatures decreased and the water content was reduced. To check air cooler performance, two studies of temperature and pressure data were made starting at 15:07 and 17:04, when the PRV was closed (no steam being dumped to containment). These studies indicate that about 85% of the water vapor removed in 87 min had been removed in 42 min (see Figure 3-4). Therefore, when the PRV had been closed for 42 min, the water vapor fraction in the containment was only about 15% higher than that in the water-saturated-air leaving the air cooler. Table 3-2 summarizes containment gas and water vapor conditions and quantities. The table indicates that at 04:00, prior to turbine trip, 2,073 kg (4,561 lb) moles of dry gas are calculated to have been in containment. At 13:50, just prior to the hydrogen burn, 2,261 kg (4,974 lb) moles of dry gas are calculated to have been in the containment, a difference of 188 kg (413 lb) moles. Correcting for about 2.7 kg (6 lb) moles of fission gas, about 185 kg (407 lb) moles of other gas, presumably hydrogen, had been added. This indicates that 7.9% hydrogen on a wet (3.5% water vapor) basis was present in containment just prior to the hydrogen burn. Subtracting the previously calculated 6.8% hydrogen burned, 1.1% hydrogen would have been in containment after the hydrogen burn.

3.2.3 Gas Depletion

Gas depleted from the containment atmosphere by the hydrogen burn is calculated to be 214 kg (471 lb) moles. This number is the difference between the gas inventories before and after the burn, as listed in Table 3-2, plus the 10 kg (23 lb) moles of gas estimated to have been discharged from the RCS to containment when the PRV was open between 14:00 and 15:07. Two-thirds of this would have been hydrogen and one-third oxygen. Therefore, this method indicates that 142 kg (314 lb) moles of hydrogen were removed during the hydrogen burn. This is 6.1% on a wet basis, which is 0.7% lower than the 6.8% previously calculated. Both methods appear to be quite accurate and, therefore, this 0.7% hydrogen difference is difficult to explain. From a hydrogen balance and the other methods of calculation, the higher value is considered to be closest to the actual value.

3.2.4 Pressure Rise Rate and Flame Velocities

Determining hydrogen concentrations from the rate of pressure rise and flame propagation velocities is qualitative at best. The rate of pressure rise is not only dependent on the hydrogen percentage, but also on the size, shape, vertical-to-horizontal orientation of the vessel, the number of compartments and barriers, sizes and numbers of openings,

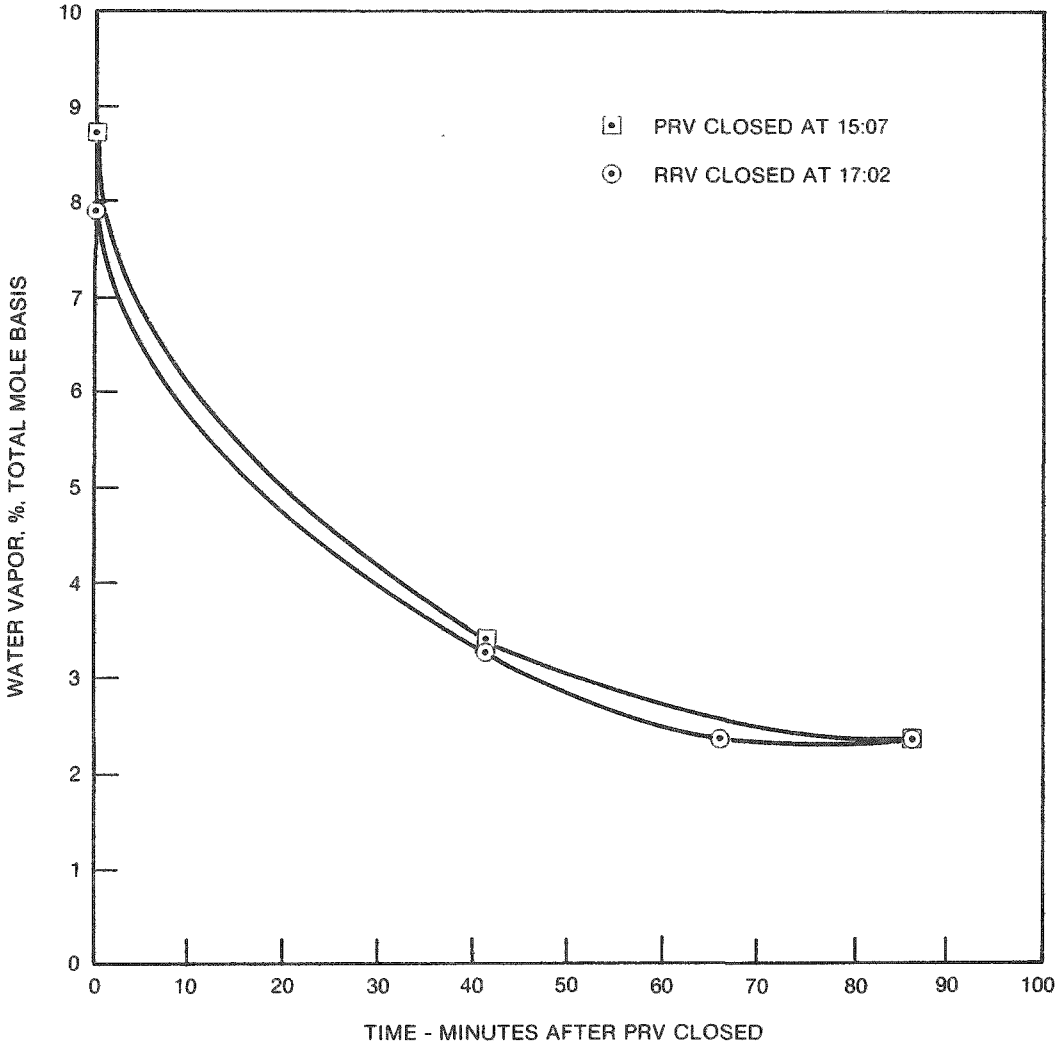

FIGURE 3-4. Percentage Water Vapor as a Function of Time after PRV Closes.

TABLE 3-2. Quantities of Gas and Water Vapor in Containment at Selected Times.

Date	Time	Temperature (°F)[a]	Pressure (psig)	n[b] total wet lb moles	Gas cooler outlet[c]		Gas pressure (psia)	n-dry gas		% water vapor (wet basis)	Comments
					Temperature (°F)	Vapor pressure (psi)		Calculated lb moles[b]	Corrected lb moles[d]		
Preburn											
03/28/79	0400	128	-0.20	4,741	82	0.55	13.95	4,561	4,561	3.9	Before turbine trip V = 2,063,000 ft^3
	0620	143	+2.20	5,310	--	--	--	--	~4,590	13.6	PRV closes
	0713	130	+0.40	4,849	90	0.75	14.35	4,608	4,590	5.3	53 min after PRV closed
	0900	157	+4.30	5,835	--	--	--	--	~4,735	18.9	Maximum pressure from steam release
	1308	135	+2.60	5,509	--	--	--	--	4,974	9.7	PRV closes
	1350	128	+1.30	5,156	78	0.47	15.53	5,004	4,974	3.5	42 min after PRV closed V = 2,033,000 ft^3 (water added)
Postburn											
	1507	138	+0.95	4,959	--	--	--	--	4,526	8.7	PRV closes
	1549	127	-0.20	4,680	72	0.39	14.11	4,554	4,526	3.4	42 min after PRV closed
	1634	124	-0.40	4,639	69	0.35	13.95	4,526	4,526	2.4	87 min after PRV closed
	1704	131	+0.65	4,921	--	--	--	--	4,533	7.9	PRV closes
	1746	124	-0.25	4,688	71	0.38	14.07	4,564	4,533	3.3	42 min after PRV closed
	1810	123.5	-0.40	4,643	68	0.34	13.96	4,533	4,533	2.4	66 min after PRV closed
	1830	121.5	-0.45	4,643	67	0.33	13.92	4,535	4,535	2.4	86 min after PRV closed
03/29/79	e	103	-0.90	4,644	61	0.27	13.53	4,533	4,553	2.0	1 day after burn
03/30/79	e	95	-1.10	4,643	59	0.25	13.35	4,558	4,558	1.8	2 days after burn
03/31/79	e	92	-1.10	4,668	59	0.25	13.35	4,582	4,582	1.8	3 days after burn
04/01/79	e	90	-1.15	4,668	59	0.25	13.30	4,582	4,582	1.8	4 days after burn

NOTE: PRV = pressure relief valve.

[a] Temperature at EL 353 ft (No. 12) considered to be average for containment.

[b] From gas law, n = PV/RT = 189,470 P/T for 2.033 x 10^6 ft^3 volume.

[c] Temperature and saturation vapor pressure at gas cooler outlet (No. 5 and 6).

[d] Corrected on the basis of the longer term data shown in Figure 3-4. This correction is based on the assumption that 85 min after the PRV has been closed, the % water vapor in the containment gas is the same as that at the gas cooler outlet.

[e] Near noon, but at time of minimum temperature and pressure, when they are fluctuating (apparently due to steam additions).

and initial turbulence. In test vessels, all relatively very small compared to the 57,600 m^3 (2 million ft^3) TMI-2 containment building, typical burn velocities for gases containing about 8% hydrogen are less than 1.5 m/sec (5 ft/sec). Horizontal burn velocities are much lower than vertical-upward velocities. Flames do not propagate downward in a quiescent atmosphere for hydrogen concentrations below 9% in air. Turbulence increases downward propagation, but velocities are low, depending on the amount of turbulence. Since pressure data indicate that the hydrogen burned in approximately 15 sec, with most of the burn occurring in less than 6 sec, it can be inferred that the burn path was predominantly from the bottom up. Even so, for a burn extending vertically almost 60 m (200 ft) and horizontally about 30 m (100 ft) burn velocities were higher than those typically measured in small vessels. The initial turbulence created by flow from the air coolers, and the "chimney" effect caused by a vertical burn in such a large and particularly tall containment would create high vertical velocities. The turbulence would also increase the horizontal velocity component. While the compartments below elevation 305 would inhibit horizontal flame propagation, the relatively open area between elevations 305 and 347, the many openings through the floor at elevation 347, and the high open bay above elevation 347 would result in high velocities, particularly upward, but also laterally and even downward in the unburned areas.

To further develop the burn speed and path, it is noted that the PRV was opened at some time between 13:49:05 and 13:49:35 as indicated by the alarm printer. (The PRV outlet temperature went "high" at that time.) The PRV was closed shortly after the containment pressure spike was observed at 13:50:27. This gas was discharged through the reactor-coolant drain-tank rupture-disk vent-line below elevation 305 near the west side of the containment. The primary upward flow path from there is through the open stairwell No. 1. Therefore, this low density steam-hydrogen plume would flow primarily up the open stairwell to the top of the containment building. This resulted in a region of higher hydrogen concentration at all levels near the open stairwell.

There are a number of evidences that the hydrogen burn occurred below elevation 305. The most convincing of these are calculations which show that the temperatures monitored there after the hydrogen burn were higher than they could have been if heated only by the supply air which had just passed through the air coolers. Further, those temperatures indicate a consistent trend with the other higher elevation temperatures, as shown in Figure 3-5.

An indication that the hydrogen burn was initiated at some point below elevation 305 and on the west side of containment is that the pressure rise recorded for OTSG A, located on the west side below elevation 305, rose in pressure 3 sec sooner than its identical twin, OTSG B, located in a compartment on the far east side of containment below elevation 305. Even though the sensor inlet location for OTSG B may have been under water at the time, calculations backed by water flow measurements through the screen at the bottom of the instrument show that its delay would have been less than 0.2 sec with a pressure lag or negative error of less than 0.5 psi as a result of having its reference opening under water.

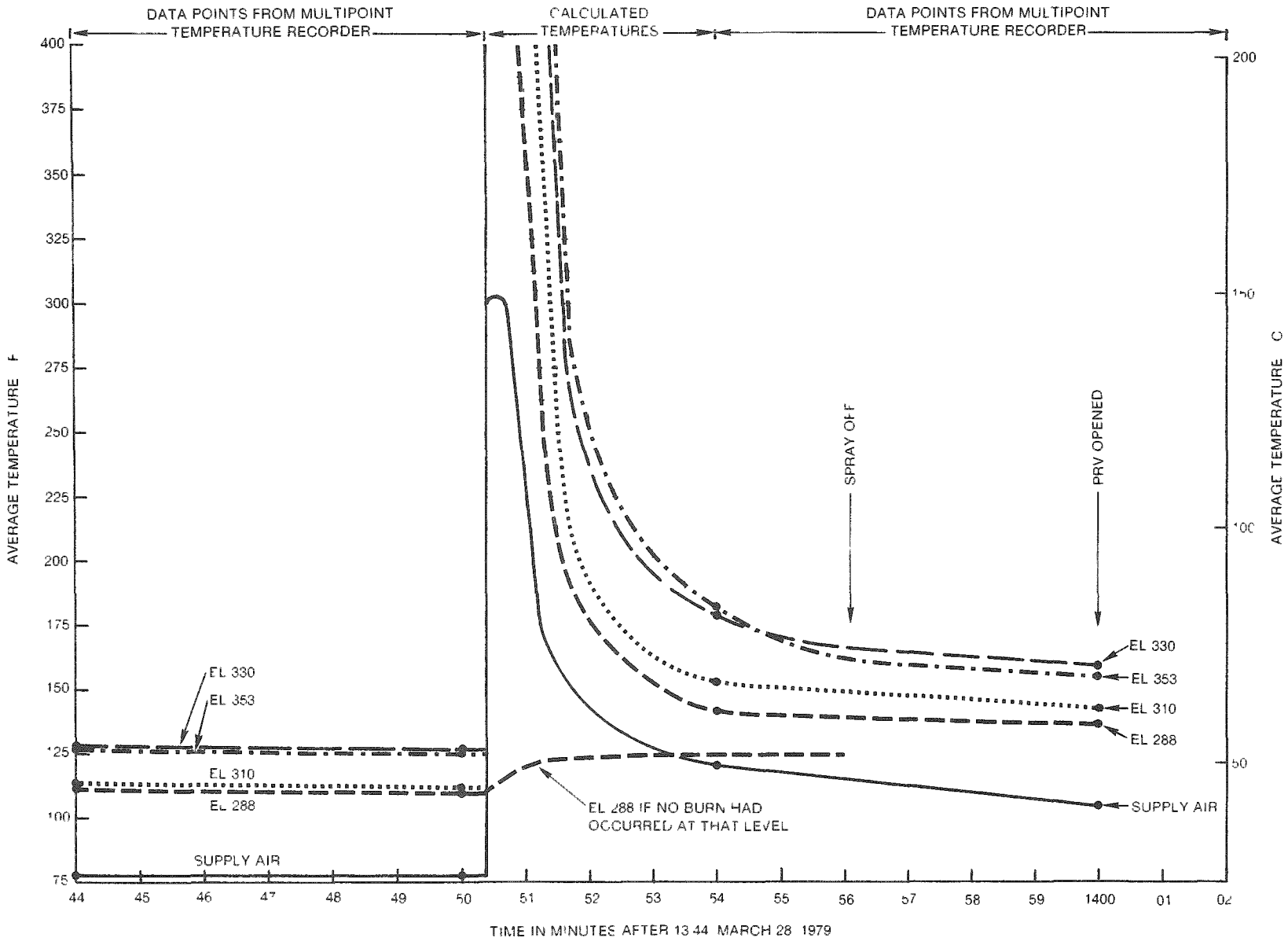

FIGURE 3-5. Average Ambient Temperature at Various Elevations Versus Time.

The pressure lag in the east compartment below elevation 305 is also shown by pressure switch BSPS 3573 (which has its pressure sensing point in that area) being the last of 10 pressure switches, nominally set to trip at 24.7 kPa (3.58 psia), to be actuated. The other nine pressure switches have pressure sensing points in the large open area on the east side of containment above the floor at elevation 305. This supports the hypothesis that at least some of the indicated OTSG pressure lag appears to be real and that the burn origin was in the compartment at the lower west side of the containment.

Four temperature alarms monitored by the plant computer (see Table 3-3) show that the hydrogen burn occurred in both D-rings.

During the first 6 or 7 sec, while the pressure was still relatively low, the burning gases were expanding as in open, relatively constant pressure burning. Resulting flame temperatures were considerably lower than for constant-volume complete burning. Correspondingly, the large volume of unburned gas was increasing in temperature as a result of compression heating. This compression heating continued until the burning stopped. When about half of the hydrogen had been burned, the absolute pressure in the containment had doubled, and the temperature of the unburned gas had increased from the 53°C (128°F) average initial temperature to 122°C (252°F). Near the end of the burn when the absolute pressure was approaching 3 atmospheres, compression heating would have increased the unburned gas temperature to 168°C (335°F). See Appendix for more detail. In the large open volume above elevation 347, radiant heat transfer from the burned gas to the unburned gas might have been even more significant. With the increased preheating, turbulence resulting from compression and convection currents, and the growing size of the flame front at all levels, the ability for the gas to burn laterally and downward would be continually increasing. Analysis of the pressure spike indicates that the last one-half of the gas to burn, compressed to one-fourth of the containment volume, burned in less than 3 sec.

First intuition might be to say that from the high pressure rise rate, with flame velocities apparently above 9 m/sec (30 ft/sec) for much of the last 6 sec, the hydrogen concentration must have been over 9% or 10%. However, considering the entire burn, which occurred in approximately 15 sec, the compression and radiant preheating, turbulence and induced flow from the gas cooler system, the locally hydrogen-enriched plume moving up the stairwell with its turbulating action, and with the tall chimney effects caused by natural convection in the high open-burning region, it appears that the burn could have occurred as rapidly as it did in a hydrogen concentration as low as the previously calculated 7.9% on a wet basis (8.2% on a dry basis).

3.2.5 Oxygen Depletion

The oxygen depletion method assumes, as a preburn condition, that the containment atmosphere is air with added hydrogen. During a hydrogen burn, hydrogen and oxygen on a 2 to 1 ratio are converted to water.

TABLE 3-3. Temperature Data Related to Burn Path.

Computer input number	Instrument abbreviation	Elevation (ft)	Angle degrees from north	Radius (ft)	Actuation		Comments
					Time hr:min:sec*	Temperature (°F)	
0403	RVIA	355	250	30	13:50:35	204	Pressurizer relief valve outlet temperature sensors are clamp-on type E thermocouples apparently exposed to the ambient air.
0404	RVIB	355	250	30	13:50:35	205	
0422	RCPIA	327	300	40	13:50:36	157	Reactor coolant pump motor inlet air temperature sensors are Minco 100 ohm platinum dual RTDs.
0425	RCPIB	327	60	40	13:50:36	125	

*Actual times of events were 0 to 30 sec prior to the time shown.

Therefore, a postburn analysis of the oxygen can be used to determine the amount of hydrogen lost. This method of calculating the amount of hydrogen burned is only as good as the oxygen analysis data available. Unfortunately, the oxygen data obtained after the TMI-2 hydrogen burn does not show good consistency. The results of two analyses of a containment gas sample taken at 0600 on 03/31/79 and the average of five samples taken on 04/01/79 are shown in Table 3-4. It is not known which are the best data. It was reported at the time that sampling procedures were changed after the first day to minimize exposure to those taking the samples. Also, an air leak in the sampling system is suspected. Assuming that the hydrogen burned from 8.2% (dry basis) down to 1.1%, the resulting gas balance would be as shown in Table 3-4.

TABLE 3-4. Gas Balance, Burning from 8.2% Hydrogen in Air (Dry Basis) to 1.1% Hydrogen, and Postburn Gas Analyses.

	Oxygen	Hydrogen	Nitrogen	Total
Air - Initial condition	0.210	--	0.790	1.000
Hydrogen/air mixture	0.193	0.082	0.725	1.000
Removed during burning	0.036	0.072	0	0.108
Postburn				
Remaining fraction	0.157	0.010	0.725	0.892
Remaining %	17.6	1.1	81.3	100.0
Analyses (%)				
03/31/79	16.1	1.7	82.2	100.0
03/31/79[a]	16.2	1.1	82.7	100.0
04/01/79	18.8	2.2	79.0	100.0
04/01/79[b]	19.0	1.1	79.9	100.0

[a]Corrected back to postburn condition by removing 0.6% hydrogen estimated to have been added to containment when the PRV was open shortly after the hydrogen burn.

[b]Corrected back to postburn condition by removing 1.1% hydrogen, which includes 0.5% hydrogen added to containment during 03/31/79 and 04/01/79.

Since the 03/31/79 gas analysis shows lower oxygen than the projected postburn condition, and the average of the 04/01 gas analyses and a number of analyses made on 04/02 and 04/03 show higher oxygen than projected, there appears to be no reason to modify earlier conclusions

based on this oxygen depletion analysis. However, the many high oxygen analyses cause one to consider that a significant fraction of the hydrogen may have been generated by radiolysis, which would also have produced oxygen.

4.0 POSTBURN TEMPERATURE DISTRIBUTIONS

The temperature-time history of gas in the postburn atmosphere plays a key role in determining burn damage. The containment average temperature-time history is shown in Figure 3-2. The following analyses were made to determine how rapidly cooling should be expected and to illustrate how the temperature-time history varied in various containment regions.

4.1 HEAT REMOVAL BY AIR COOLER

Each of the regions of the containment is ventilated by cool air supplied by the air coolers. The purging of cool air through a gas space represents a mechanism which controls heat removal in the long term, but is minor compared to heat transfer to surfaces during the first minute following the burn. Five coolers, operating at approximately 22.2 m^3/sec (47,000 ACFM) each, were on-line during and after the burn.

The performance of the coolers was computed using a heat transfer coefficient surface area product (UA) of 589 W/sec^{o}C (67,000 Btu/hr^{o}F), a water inlet temperature of 7^{o}C (45^{o}F) and a water flow rate of 380 L/sec (800 gal/min) for each cooler. Calculated steady state outlet temperatures are listed in Table 4-1.

TABLE 4-1. Predicted Outlet Temperature of Air Coolers, Steady State.

Gas inlet temperature		Gas outlet temperature	
^{o}C	^{o}F	^{o}C	^{o}F
704	1300	188	370
649	1200	173	344
593	1100	159	318
538	1000	144	292
427	800	116	240
316	600	88	190
204	400	59	138

Transient calculations that accounted for the thermal inertia of cooling water [2270 kg (5,000 lb total inventory)] and copper coils and fins [11,800 kg (26,000 lb total inventory)] showed that peak gas outlet temperatures were approximately 149^{o}C (300^{o}F), or some 39^{o}C (70^{o}F) below the maximum predicted for steady state.

The heat removal rate due to coolers may be estimated as the product of $mC_p\Delta T$ where

m = mass flow rate, kg/sec (lb/sec)

C_p = gas heat capacity at constant pressure, J/kg·K (Btu/lb^{o}F)

ΔT = temperature difference across the cooler, ^{o}C (^{o}F).

The air flow rate to each of the containment regions, as designed and as estimated on the basis of duct area leaving the coolers, is shown in Table 4-2. Approximately 66% of cooler output was directed to the D-rings, making heat removal by air coolers most important for this region.

TABLE 4-2. Flow Areas of Ducts Leaving Air Cooler.

Duct description	Duct diameter, in.	Flow area, ft^2	Fraction of total flow area (%)	Design flow rate	Fraction of total flow (%)
D-ring					
East	72	28.3	0.70	79,210	0.66
West	84	38.5		65,810	
Elevation 282					
East	40	8.7	0.10	23,840	0.11
West	8	0.4		1,140	
LOCA Duct					
East	42	9.6	0.20	25,000	0.23
West	42	9.6		25,000	

4.2 HEAT TRANSFER TO EXPOSED SURFACES

The dominant heat loss mechanism from postburn gases (prior to spray operation) is transfer to exposed surfaces. In general, the loss rate can be expressed as follows:

$$q = hA(T_g - T_s) \qquad (2)$$

where

q = heat loss rate, watts (Btu/sec)

h = heat transfer coefficient, $w/m^2 \cdot K$ (Btu/sec^oF ft^2)

A = exposed surface area, m^2 (ft^2)

T_g, T_s = temperature of gas and surface, respectively.

The cool-down rate of gas in a compartment is related to q by

$$\frac{dT}{dt} = - \frac{q}{mC_v} \qquad (3)$$

where

$\frac{dT}{dt}$ = gas cool-down rate, ^oC/sec (^oF/sec)

m = mass of gas in the compartment, kg (lb)

C_v = heat capacity at constant volume, J/kg·K (Btu/lb^oF).

Surface areas for heat transfer and gas volumes were estimated from engineering drawings of the Unit-2 plant. The overall containment was divided into three regions. Areas and volumes for these regions are given in Table 4-3.

The data presented in Table 4-3 illustrate the importance of realistically accounting for surface areas in containment. The total surface is estimated to be approximately 2.7 times greater than that of the steel containment liner. Another important point is that the region below elevation 347 has a surface/volume ratio some four times larger than that in upper containment. The equipment areas listed in Table 4-3 are thought to err on the low side; future detailed studies might be useful to arrive at more precise estimates of equipment surface areas in containment.

Heat transfer from the gas to its surroundings would result from both radiation and convection. The approach used here was to derive overall heat transfer coefficients from hydrogen burn tests carried out at Rockwell.[1] The variation of h with gas temperature, deduced from small-scale test data, is portrayed in Figure 4-1. The heat transfer coefficients displayed in Figure 4-1 increase rapidly with temperatures above 538^oC (1000^oF). This is thought to be the result of radiation.

Condensation per se has little effect on sensible heat (temperature) loss from the gas, however, the quantity of heat removed by condensation is probably significant. Condensation heat transfer effects could not be readily segregated from the Rockwell[1] test data and were, therefore, included implicitly in the cool down analyses.

TABLE 4-3. Heat Transfer Surface Areas and Gas Volumes in Three Containment Regions.

Heat transfer area	Inside D-rings	Below EL 347 ft	Above EL 347 ft	Total containment
Uninsulated equipment, Kft^2	17	39	34	90
Painted steel liner, Kft^2	3	55	77	135
Concrete, Kft^2	35	84	26	145
Total uninsulated area, Kft^2	55	178	137	370
Gas volume, Kft^3	211	428	1,394	2,033
Surface/volume, ft^{-1}	0.26	0.42	0.10	0.18

NOTE: EL = Elevation.

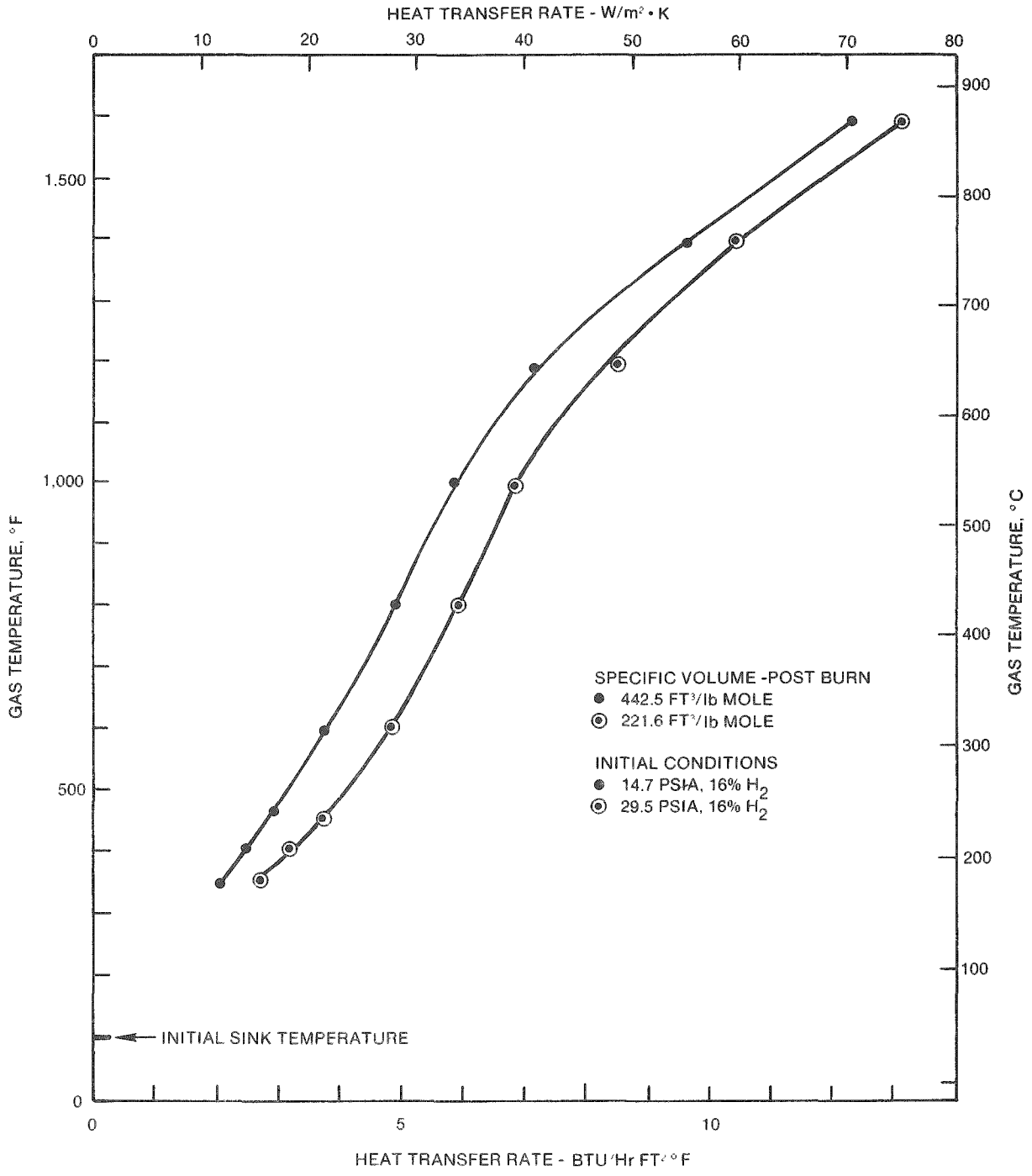

FIGURE 4-1. Overall Heat Transfer Rate Versus Gas Temperature for Different Gas Mixtures. (From Reference 1, Figures 12 and 14.)

4.3 PREDICTED DECAY OF POSTBURN GAS TEMPERATURES

The time-temperature history for the three containment regions described in Table 4-3 was predicted using Equations 2 and 3 along with the areas of Table 4-3 and heat transfer coefficients for the containment atmosphere specific volume and the curves shown in Figure 4-1.

Initial temperatures in each volume were established from theoretical calculations of an adiabatic burn. From the time of the theoretical burn until sprays operated, heat transfer in all three regions was computed independently. After sprays started, convection heat transfer in the lower unsprayed area was accounted for as before, but the cooling rate in the upper containment (the sprayed volume) was computed so that the predicted overall cooling rate agreed with the measured overall cooling rate.

Two cases involving different hydrogen burn assumptions were analyzed. In each case it was assumed that the containment hydrogen concentration was 7.9% on a wet basis (3.5% water vapor) and was well mixed. In the first, it was assumed that hydrogen in the region above elevation 347 burned down to 1% hydrogen; to 2% hydrogen in the D-rings; and to 2.2% hydrogen below elevation 347. This balances the total containment burning to an average of 1.1%. Results of this computation are illustrated in Figure 4-2.

As indicated by the curves of Figure 4-2, the temperatures in lower regions fall much faster than in upper containment due to higher surface/volume ratios there. The predicted average temperature agrees very well with the measured value up to spray initiation. This supports the validity of the heat transfer analysis.

A second burn case assumed complete burning in the upper region. To balance the total containment burning to 1.1%, burning in the region below elevation 347, including the region in the D-rings, would have been down to about 3.5% hydrogen. Results are shown in Figure 4-3. As indicated by the curves on this figure, these assumptions raise the upper containment temperatures and lower those below elevation 347.

These time-temperature figures illustrate the degree to which lower containment regions are comparatively cooler in the postburn atmosphere. The most obvious effect would be to minimize burn damage in these regions.

4.4 CONSIDERATION OF LACK OF COMBUSTION BELOW ELEVATION 305

A hypothetical case was analyzed to determine whether the measured gas temperatures in the containment regions below elevation 305 were consistent with the postulate that no burn occurred there. The issue is germane because the temperature recorder did not record points during the early postburn period. At about 13:54, the first postburn time when the recorder printed a gas temperature, the temperature had already decayed to within 28°C (50°F) of preburn conditions. Thus one could

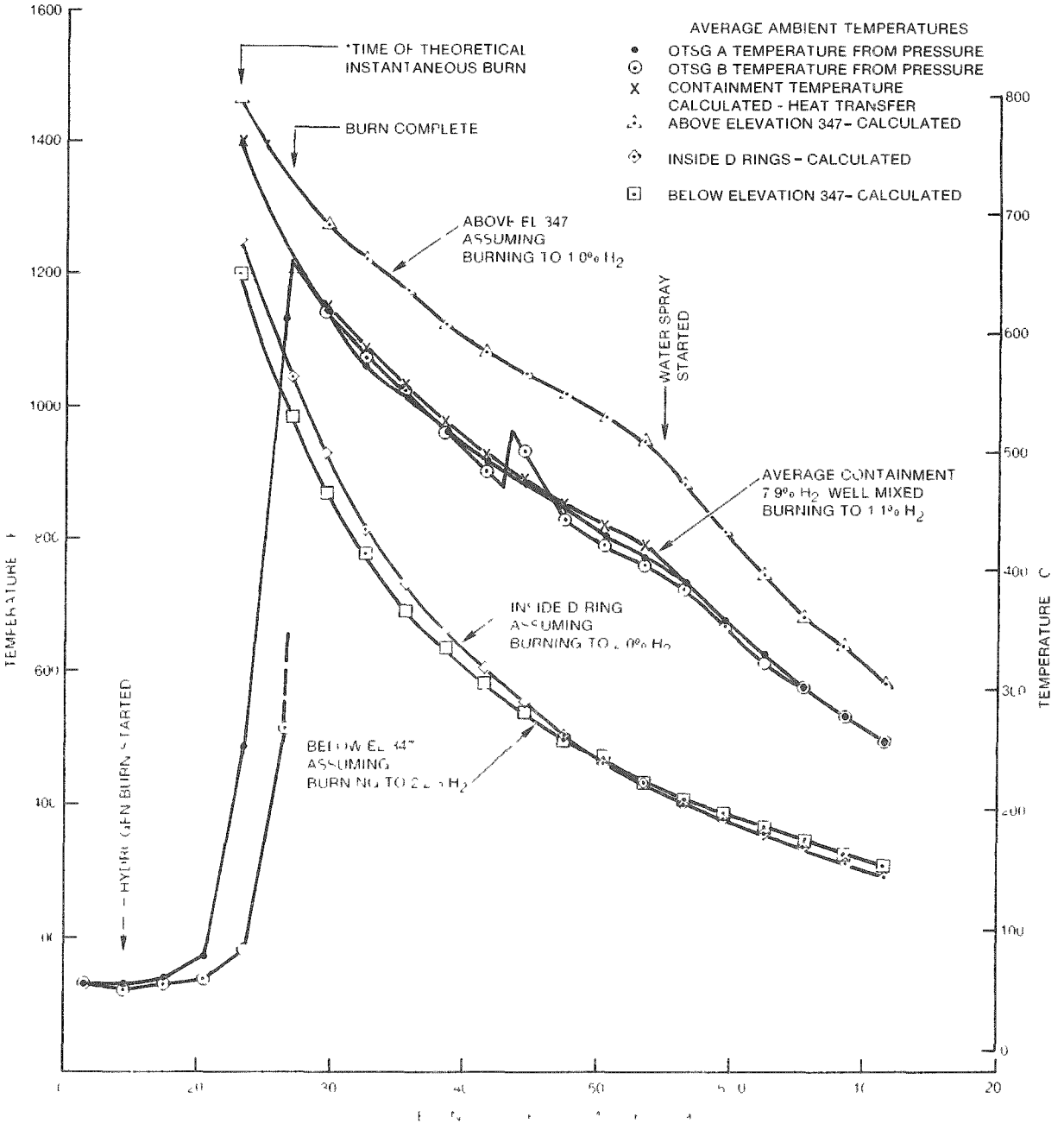

FIGURE 4-2. Average Ambient Temperature Versus Time Above and Below Elevation 347, Assuming More Incomplete Burning Below Elevation 347.

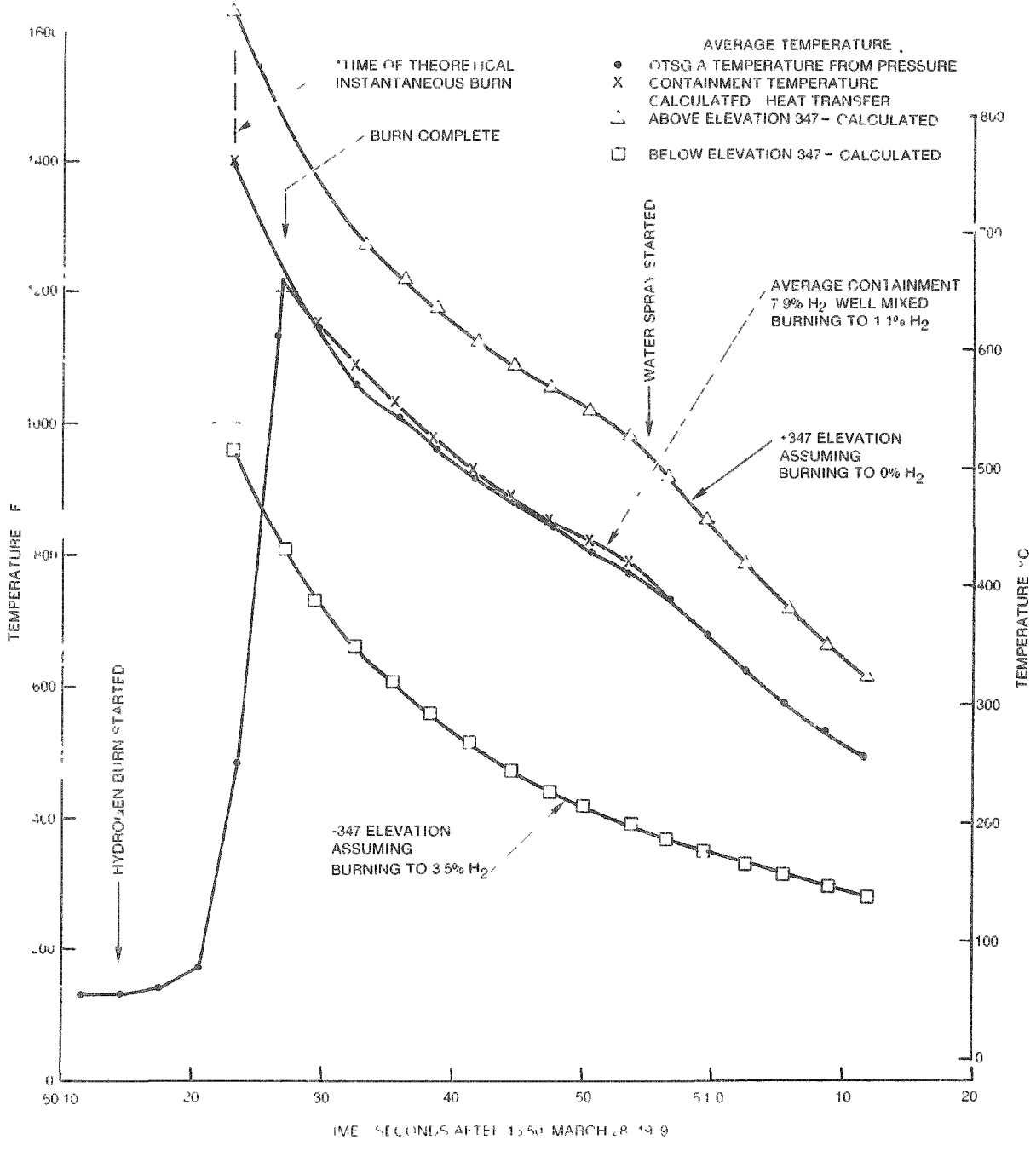

FIGURE 4-3. Average Ambient Temperature Versus Time for Total Containment Atmosphere and for Major Segments.

postulate that the modest temperature rise measured for the region below elevation 305 resulted from heating by air from containment coolers; the containment coolers would discharge air that was hotter than the initial room temperature for several minutes.

Atmospheric temperatures in the region below elevation 305 were predicted using the following key assumptions:

- Heat loss to walls and heat gain from walls was negligible
- Heat gain by compression heating equals heat loss by expansion cooling
- Gas entering the cooler inlet was at the average containment temperature
- The room was ventilated at the rate of six changes per hour
- Room air was perfectly mixed.

Predicted temperatures are compared with measured temperatures in Figure 3-5. These curves show that the temperature at elevation 288 is predicted to increase by only 8°C (15°F) at 13:54, whereas the measured temperature was 18°C (32°F) higher than the initial value. A study of potential errors in the predicted temperature increase due to the purging process indicated that the values shown in Figure 3-5 could not be low by 10°C (17°F) and, therefore, that the room could not have been heated solely by this purging process. It is inferred that a hydrogen combustion occurred in this region.

5.0 BURN DAMAGE

Numerous observations and photographs[6] taken inside the containment provide detailed information on damage that can be attributed to the hydrogen burn. Available information has been studied to see whether the observed damage is consistent with the overall picture of the burn developed herein.

5.1 TRANSIENT HEATING OF MATERIALS IN A HYDROGEN BURN

As was illustrated in Section 4.0, the hydrogen burn imposed a brief temperature and pressure spike on the containment atmosphere. The temperature profile in a dry exposed material body depends on the following factors:

- Heat flux at exposed surface (a function of time)
- Thermal diffusivity of the material
- Material thickness
- Time.

The heat flux imposed on surfaces in TMI-2 resulted from radiative and convective heat transfer. For postburn gases composed of 10% water vapor, the product of water vapor pressure and path length is on the order of 10 atm-ft for the upper containment, yielding an emissivity of approximately 0.47 at 760°C (1400°F) and 0.56 at 200°C (400°F).[7] For compartments having equivalent diameter of 20 ft, the product of path length and vapor pressure would be approximately 2, yielding emissivities of approximately 0.3 at 760°C (1400°F). A comparison of calculated radiant heat transfer rates to the measured total heat transfer rates (derived from Figure 4-1) indicates that in the upper containment, radiant heat transfer accounts for 72% of the total at 760°C and 40% of the total at 200°C. In a 6 m (20 ft) compartment, radiant heat transfer would account for 43% and 24% of the total heat transfer at 760°C and 200°C, respectively.

Thermal diffusivities of materials vary markedly. Metals, like carbon steel, have high thermal diffusivities and would cause heat energy to be absorbed through a significant thickness. Materials of low thermal diffusivity are plastics and wood. These would be expected to develop large temperature gradients when exposed to hot gas. Concrete has a thermal diffusivity intermediate between those of steel and wood. Thermal diffusivity is defined by $K = k/\rho C_p$ where k is the thermal conductivity, ρ is density and C_p is specific heat. In summary, wood and plastics would be expected to experience relatively higher surface temperatures due to the hydrogen burn than would be experienced by structural steel.

Material thickness is obviously important; not only will heat penetrate more uniformly through a thin body, but also the body will become hotter due to its lower thermal inertia.

5.2 AFFECT OF SURFACE MOISTURE

Liquid water was undoubtly present on some surfaces just prior to the burn and would have an important effect on the final temperature reached because of heat absorbed by evaporation. Based on the time-temperature history for upper containment, it was estimated that a water film approximately 0.5 mm (0.02 in.) thick would absorb the entire heat load by evaporation. Therefore, objects that were wet by water (condensed steam from the PRV discharge) would not be heated nearly as much as similar objects that were dry at the time of the burn.

5.3 REPRESENTATIVE HEATING CALCULATIONS

The transient heat conduction equation was solved by minicomputer for a few representative cases. One-dimensional slabs, heated from one side and insulated on the other, were divided into nine equally spaced nodes and subjected to heat fluxes based on the temperature-time profiles and heat transfer coefficients discussed in Section 4.0. This is identical to heating a slab of twice the thickness from both sides. Five cases that were analyzed are described in Table 5-1. Gas temperatures were taken from Figure 4-2 with peak temperatures extended to 788°C (1400°F) in each case, above and below elevation 347.

TABLE 5-1. Heat Transfer Cases Analyzed.

Case number	Material	Thickness		Position in containment
		mm	in.	
1	Painted carbon steel	6.4	0.25	+347
2	Wood	$\geq$9.5	$\geq$0.375	+347
3	Wood	3.2	0.125	+347
4	Wood	3.2	0.125	-347
5	Wood	$\geq$9.5	$\geq$0.375	-347

Surface temperatures predicted for the five cases described in Table 5-1 are shown graphically in Figure 5-1.

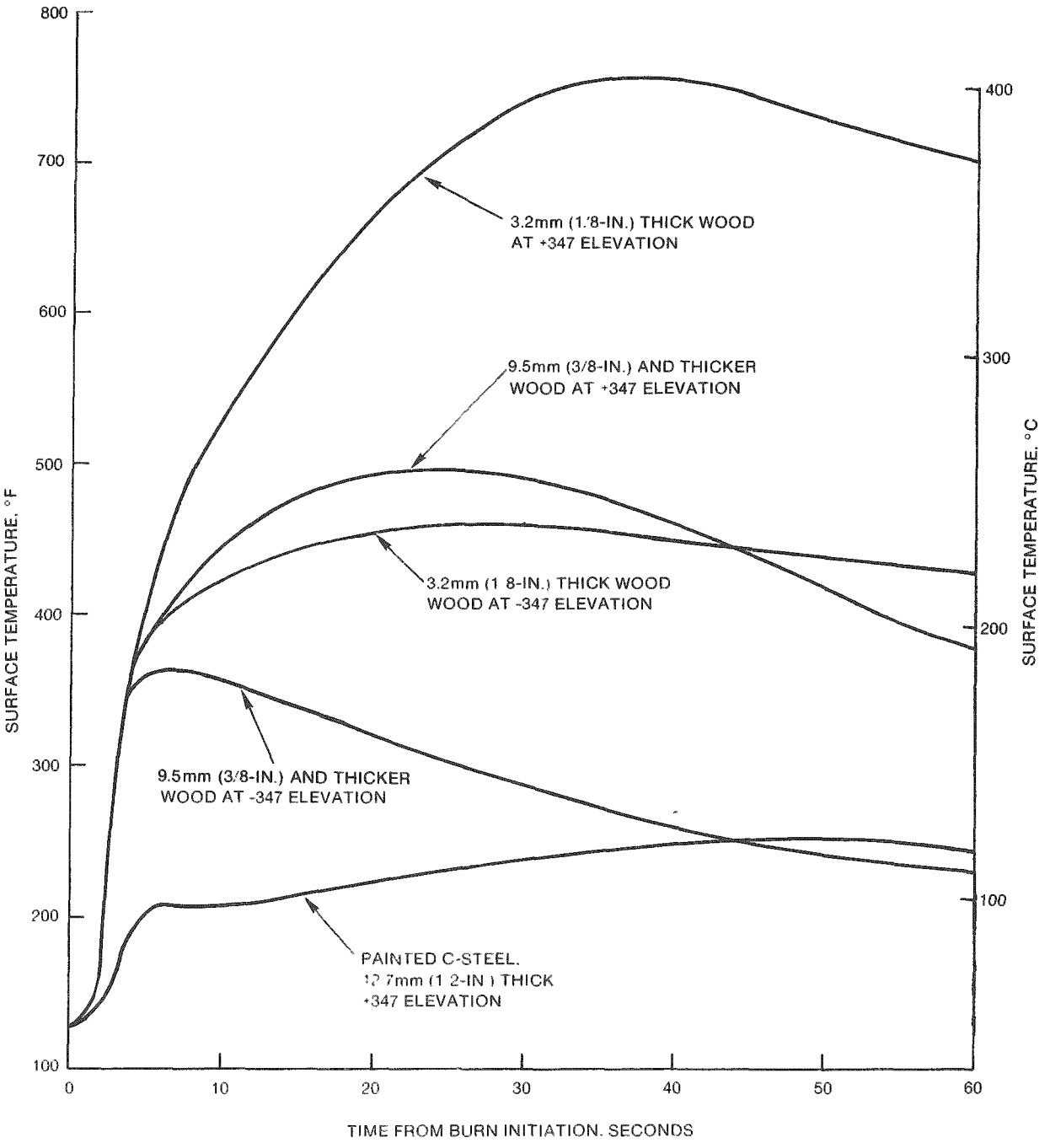

FIGURE 5-1. Surface Temperatures Predicted for Plywood and Painted Carbon Steel Exposed on Both Sides.

As indicated by the curves of Figure 5-1, the surface temperatures achieved during the 60 sec period depend strongly on material properties, thickness, and location in containment. Thin materials [3.2 mm (1/8 in. heated from both sides or equivalently 1.6 mm (1/16 in.) heated from one side] can develop much higher surface temperatures than thicker slabs of the same material. Interestingly, wood sheets thicker than 9.5 mm (3/8 in.) had the same surface temperatures. The reason is that the heat was unable to penetrate more than 4.8 mm (3/16 in.) in the 60 sec period. Therefore, thicker wood sections would exhibit the same surface temperatures shown for 9.5 mm (3/8 in.) boards.

The carbon steel slab increased in temperature much less than wood. Most of the temperature increase shown in Figure 5-1 for carbon steel actually was across the 0.25 mm (0.010 in.) layer of paint.

The lower surface temperatures achieved by wood sheets in low regions of the containment (-347 ft elevation) simply reflects the faster falloff of gas temperatures in this region. As noted in Section 4.0, the higher surface/volume ratio in lower containment regions causes the postburn temperature to decay faster in those regions. Therefore, less burn damage would be expected in lower parts of the containment than in upper regions.

Temperature profiles through three slabs at 8 sec after burn initiation are illustrated in Figure 5-2. As indicated by the curves of Figure 5-2, thin sections are heated to higher temperatures than thick ones. Large temperature gradients can develop in wood, but in steel the heat flux is too low to cause large gradients. A temperature drop of approximately 50°F is experienced across the paint [0.25 mm (0.010 in. thick)] at 8 sec, illustrating its low thermal conductivity compared to steel [0.26 W/m·K (0.15 Btu/hr°F ft) versus 45 W/m·K (26 Btu/hr°F ft)].

These calculations are presented to illustrate important aspects of transient heating of materials exposed to hot gases. The predictions would have been more accurate if the following heating/cooling effects had been accounted for:

- Heat transfer effects due to condensation of water
- Heat transfer effects due to evaporation of water
- Energy absorption due to pyrolysis of heated materials
- Energy absorption due to phase changes of heated materials
- Energy addition due to combustion.

5.4 DISCUSSION OF OBSERVED BURN DAMAGE

A first generalization that should be stated is that overall, little apparent damage to the containment was caused by the hydrogen burn. Massive structures appear largely unaffected; noticeable damage is confined to thin organic-based materials, such as plastics, paper, and wood.

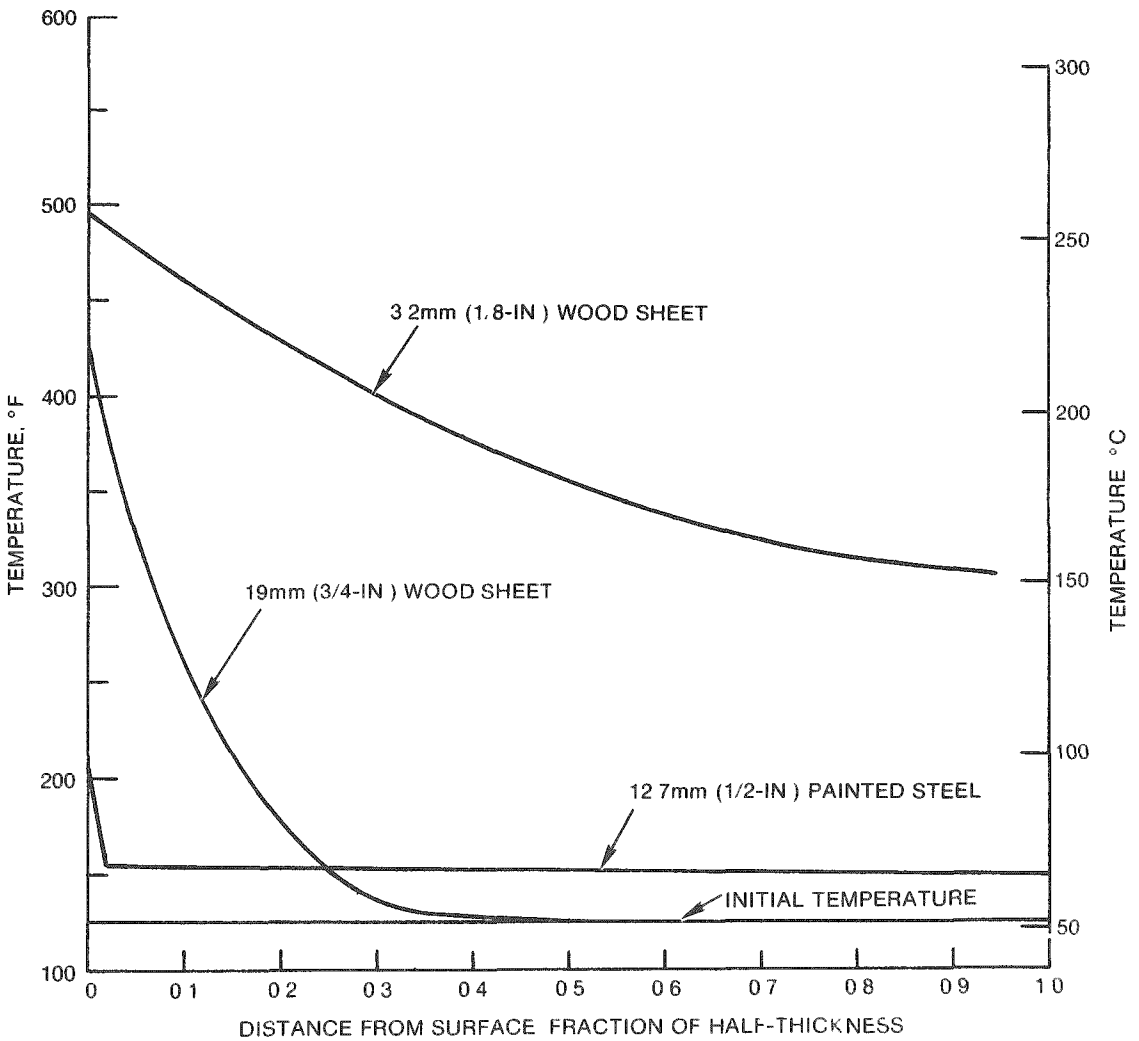

FIGURE 5-2. Temperature Profiles 8 sec After Burn Computed for Materials in Upper Containment Being Heated from Both Sides.

The effect of elevation in the containment is illustrated in Figures 5-3 and 5-4. The telephones shown in these two photographs are from elevations 347 and 305, respectively. The significantly greater damage at 347 is consistent with the higher gas temperature history (time and temperature) at the higher elevation. Note that the cord on the telephone at elevation 305 (Figure 5-4) has suffered damage, indicating that an appreciable temperature spike occurred at that level. Also note that the section of the coiled cord on the table adjacent to the phone in Figure 5-3 appears to be undamaged, except for slight scorching at the top of each coil. This demonstrates that temperatures are lower where convection currents are minimized and the heat-transfer-surface-area to gas-volume ratio is high.

Discussions with TMI personnel have indicated that burn damage appears to vary with the angular position in the containment at elevations 305 and 347, with least damage being seen on the westward side. This observation is explainable in terms of wetness in this region. Steam released from the PRV apparently entered upper containment volumes through the open stairway (No. 1) located on that side. The steam left the RCDT in a saturated state and would have wet cool surfaces by condensation. Indeed, temperature sensor 13, which is located in the vicinity of the stairway, and sensor 6, which is located at the west end of the air cooler, exhibited significant subcooling after each PRV closure. This subcooling is indicative of a condensed water film deposited during steam discharge periods. Because liquid water would suppress temperature rises of materials, burn damage would be a strong function of local wetness. Generally, the region near the No. 1 stairway (west side) would be expected to be most protected by water, and this is consistent with the observations.

Figures 5-5 and 5-6 illustrate local damage effects that are consistent with expectations. In Figure 5-5, wooden scaffolding boards (at elevation 347) are shown from below, and indicate a minor degree of charring. Tape that held the plastic protected the wood, leaving the unburned marks. In Figure 5-6, a manual is charred mainly on upper parts which were exposed to hot gas. The lower part, which was in contact with a steel box, apparently suffered less damage. Both of these examples are consistent with heating over a brief time period.

Mechanical damage caused by the pressure pulse was minimal. However, as shown in Figure 5-7, 55-gal drums were partially collapsed by the external pressure. Two of the drums suffered little distortion, and it can be concluded that they were either full or not sealed. Also shown in Figure 5-7 is an air duct which was not damaged by the pressure pulse. Numerous other pictures of air ducts are shown in Reference 6 and in no case is observable mechanical damage apparent. The drums were not damaged predominantly on one side or tipped over by the pressure pulse. This drum damage and lack of duct damage is consistent with a pressure pulse that developed over seconds (i.e., from a deflagration) but is not consistent with the passage of a detonation wave. This supports the view that a detonation did not take place in TMI-2.

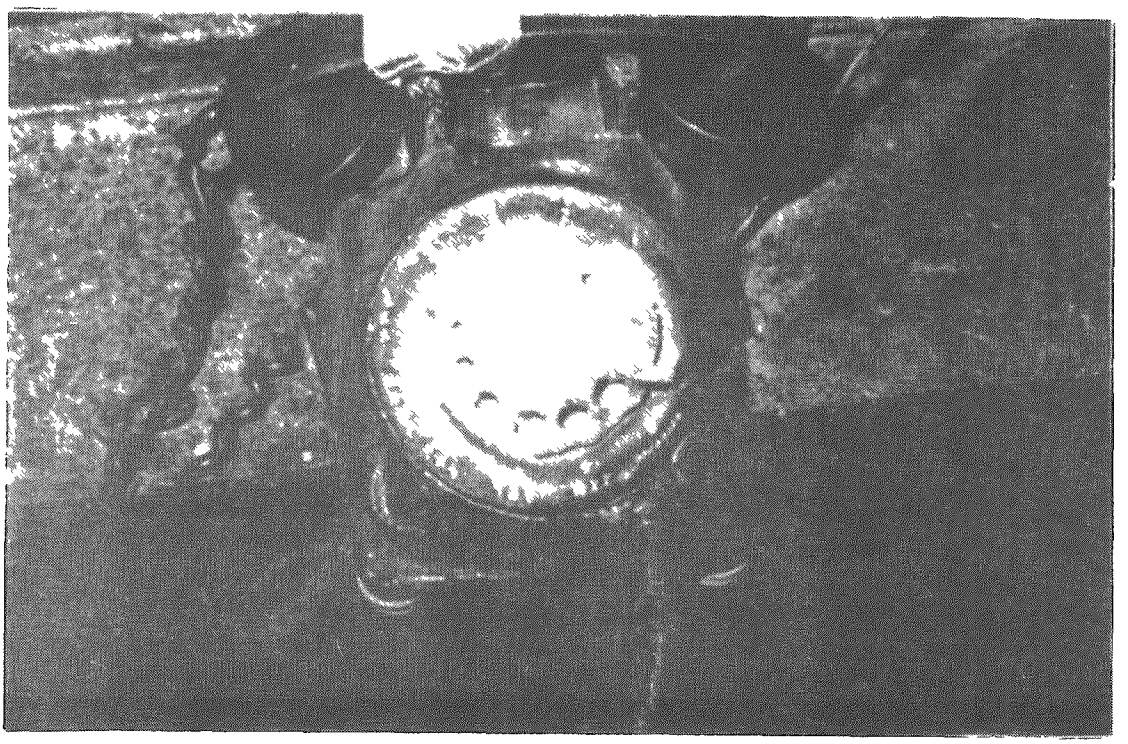

FIGURE 5-3. Close-up of Bell Telephone.

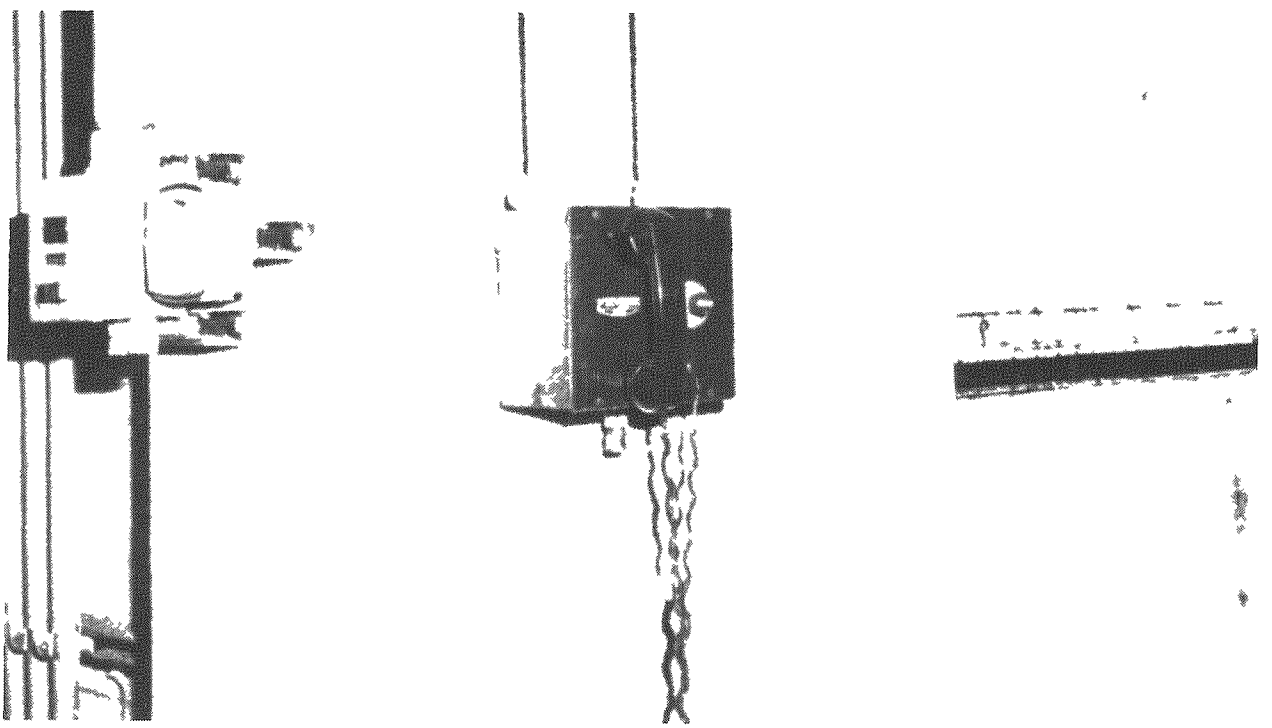

FIGURE 5-4. Gai-tronic Telephone and Elevator Door.

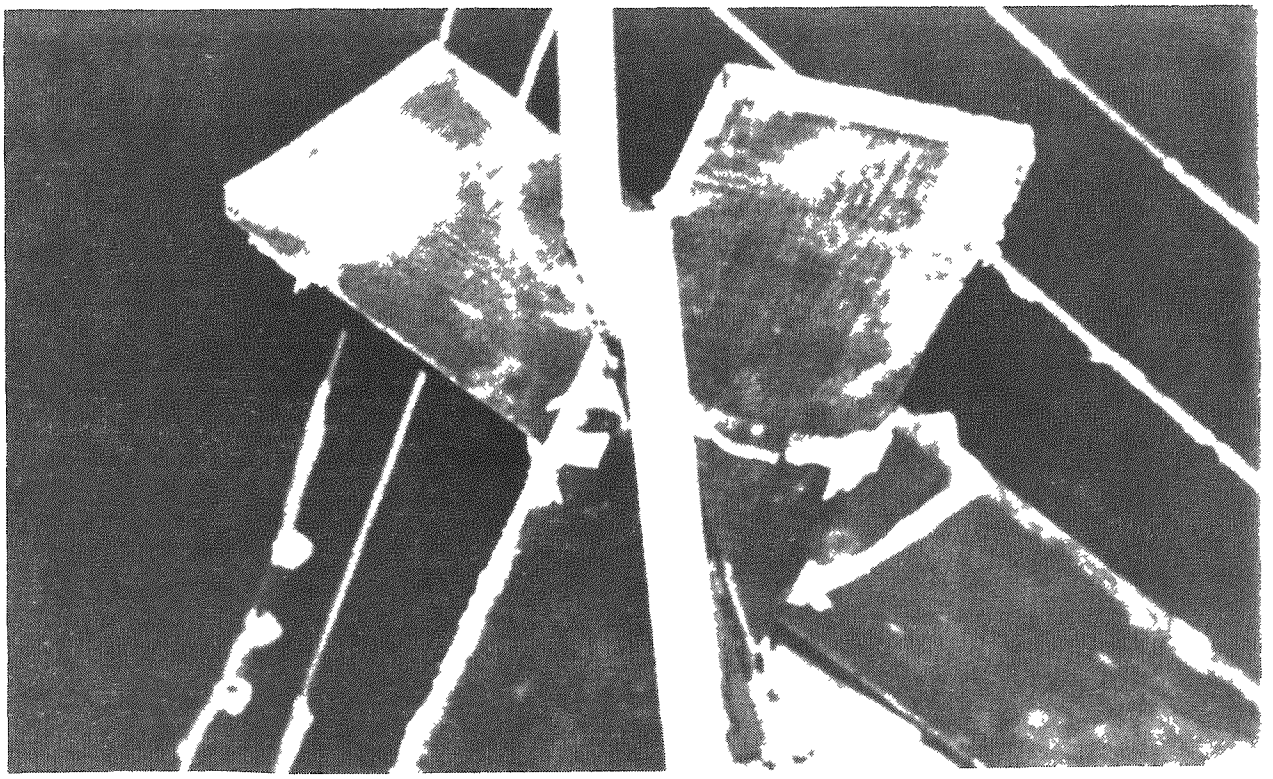

FIGURE 5-5. Scaffolding.

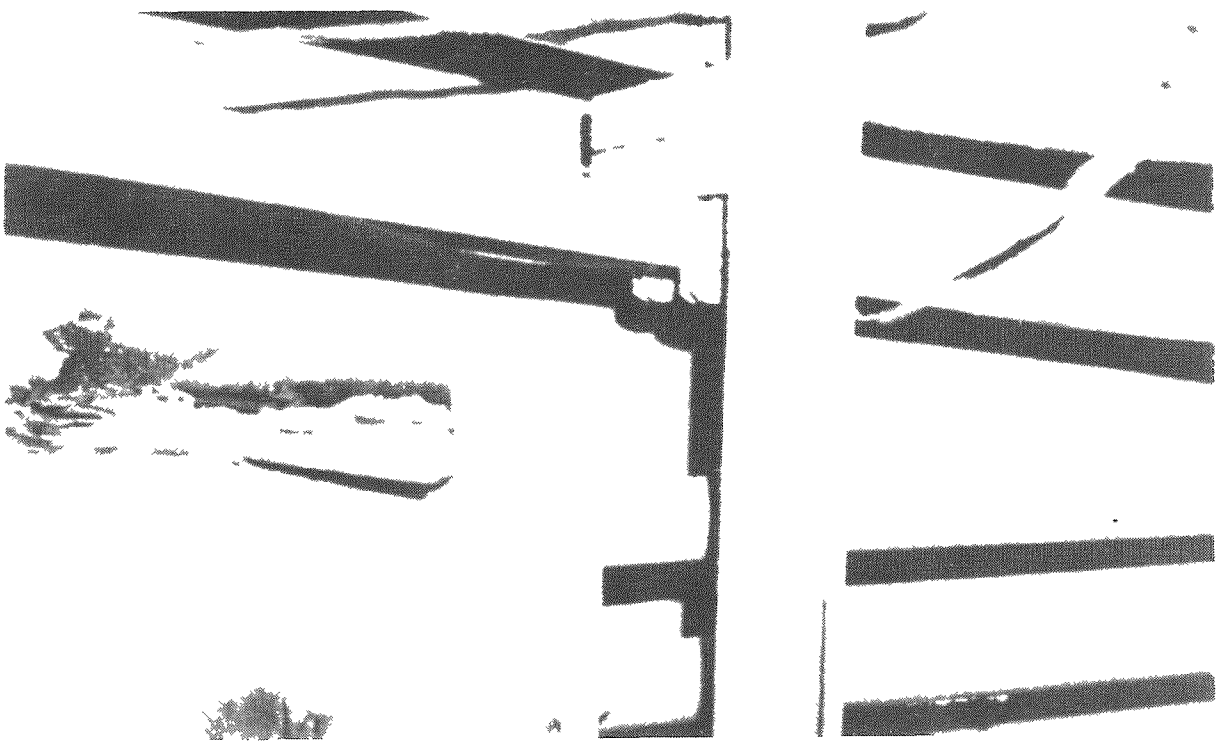

FIGURE 5-6. Charred Manual Lying on Top of Electrical Box.

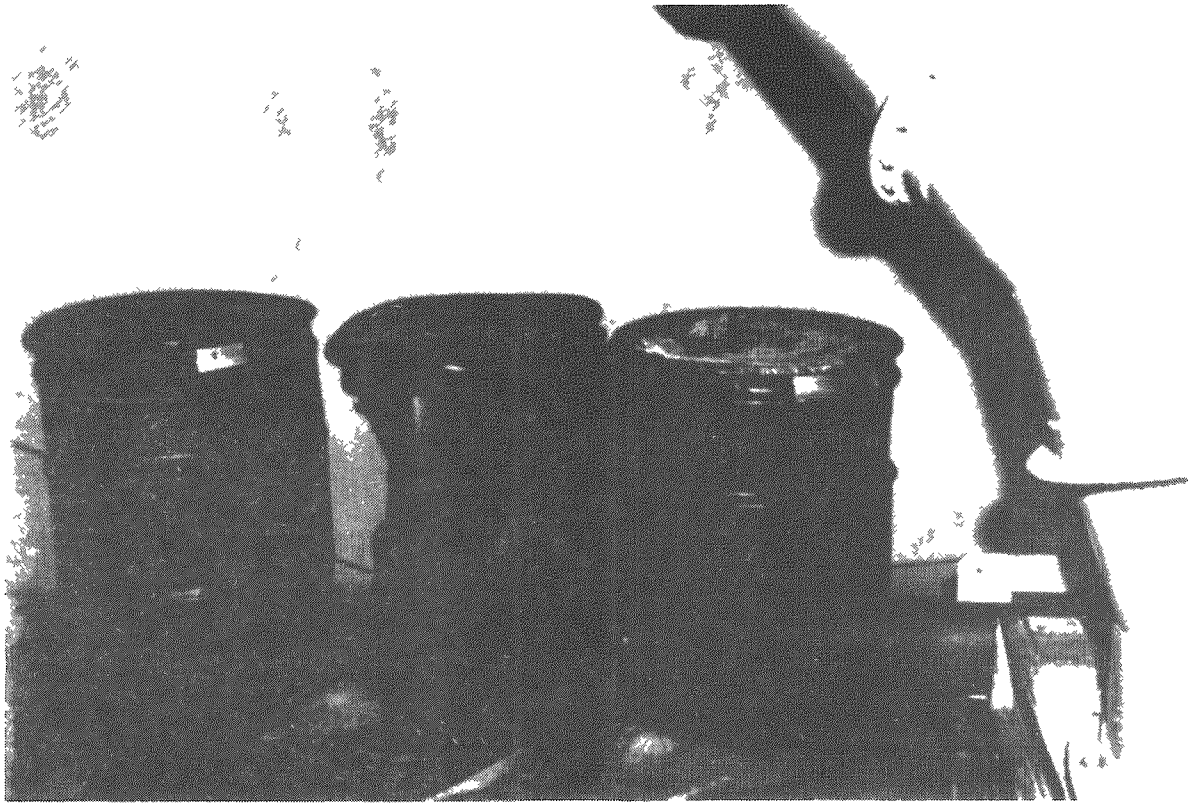

FIGURE 5-7. Fifty-Five Gallon (0.21 m^3) Drums Between Enclosed Stairwell and Air Duct.

In summary, the burn damage observed in post-accident entries appears to be fully consistent with expectations based on the burn scenario described herein. Key aspects follow.

- Higher temperatures would be expected in upper containment regions because burn efficiency was highest (radiant preheating in open volume, slightly higher hydrogen concentrations, more turbulent mixing) and cooldown was slowest (lower heat transfer area to gas volume ratio).

- Thin plastics, paper, wood, and plastic or rubber electrical insulation would be most susceptible because of the heat transfer characteristics of these materials and their ability to char or ignite. Thick sections of these materials would be much less affected.

- Surfaces wet by steam condensate (west side) would not be much affected because of energy absorbed by vaporization.

- Local geometries that would inhibit convection currents or cool the gas locally would minimize peak temperatures reached in the materials.

- Combustible materials, such as paint, in close contact with, and particularly when bonded to, good heat conductors should not have been significantly affected by the burn transient.

- The thermal transient resulted from a general burn of hydrogen, not a detonation.

6.0 POSTBURN HYDROGEN

The calculations discussed previously indicate that there was 1.1% hydrogen remaining in containment after the hydrogen burn. Most of this was probably in compartments below the 305 elevation floor, but would disperse rapidly. The pressure spike, indicated by the OTSG B pressure data at 13:50:41, appears to have been due to a relatively large afterburn below the 305 elevation floor near the east side of the containment. The pressure impulse affected the OTSG A pressure, measured about 30 m (100 ft) west of OTSG B, as a delayed wave. This delay should be expected since the D-rings and a number of compartments separate the two reference pressure sensing points.

At 14:01 the PRV was again opened for a little more than 1 hr. This opening depressurized the RCS to its lowest pressure, about 345 kPa (50 psi) lower than it had previously been that day. This caused an additional estimated 0.6% hydrogen to enter containment from the RCS. Between March 31 and April 2, another 0.5% hydrogen was transferred to containment. The thermal hydrogen recombiner developed by Rockwell International started removing hydrogen from containment on April 2 at 15:30. A plot of its operation and additional hydrogen transfers to containment are indicated in Figure 6-1. Recombiner operation was terminated on May 1 after it had removed 56 kg (123 lb) moles of hydrogen gas [and 28 kg (61 lb) moles of oxygen gas] from containment, and the hydrogen concentration was down to 0.7%. This residual hydrogen was removed from containment the following summer when it was vented to the atmosphere.

The quantities of hydrogen added to and removed from containment are summarized in Table 6-1. A calculated total of 229 kg (505 lb) moles or 459 kg of hydrogen gas entered and was removed from containment. Assuming, somewhat arbitrarily at this time, that 90% of the hydrogen was generated by the zirconium-steam reaction and 10% by radiolysis, about 410 kg or 205 kg (450 lb) moles of hydrogen gas were generated as a result of the zirconium-steam reaction.

Since 1 mole of zirconium reacting with 2 moles of water liberates 2 moles of hydrogen, 205 kg moles of hydrogen represents the oxidation of 102 kg moles or 9,300 kg (20,500 lb) of zirconium. The TMI-2 reactor core contains a calculated 18,770 kg (41,300 lb) of zirconium cladding in contact with active fuel and about 23,600 kg of zirconium total. Therefore, the zirconium oxidized is equal to about 50% of the active fuel cladding weight or about 40% of the total zirconium in the reactor core.

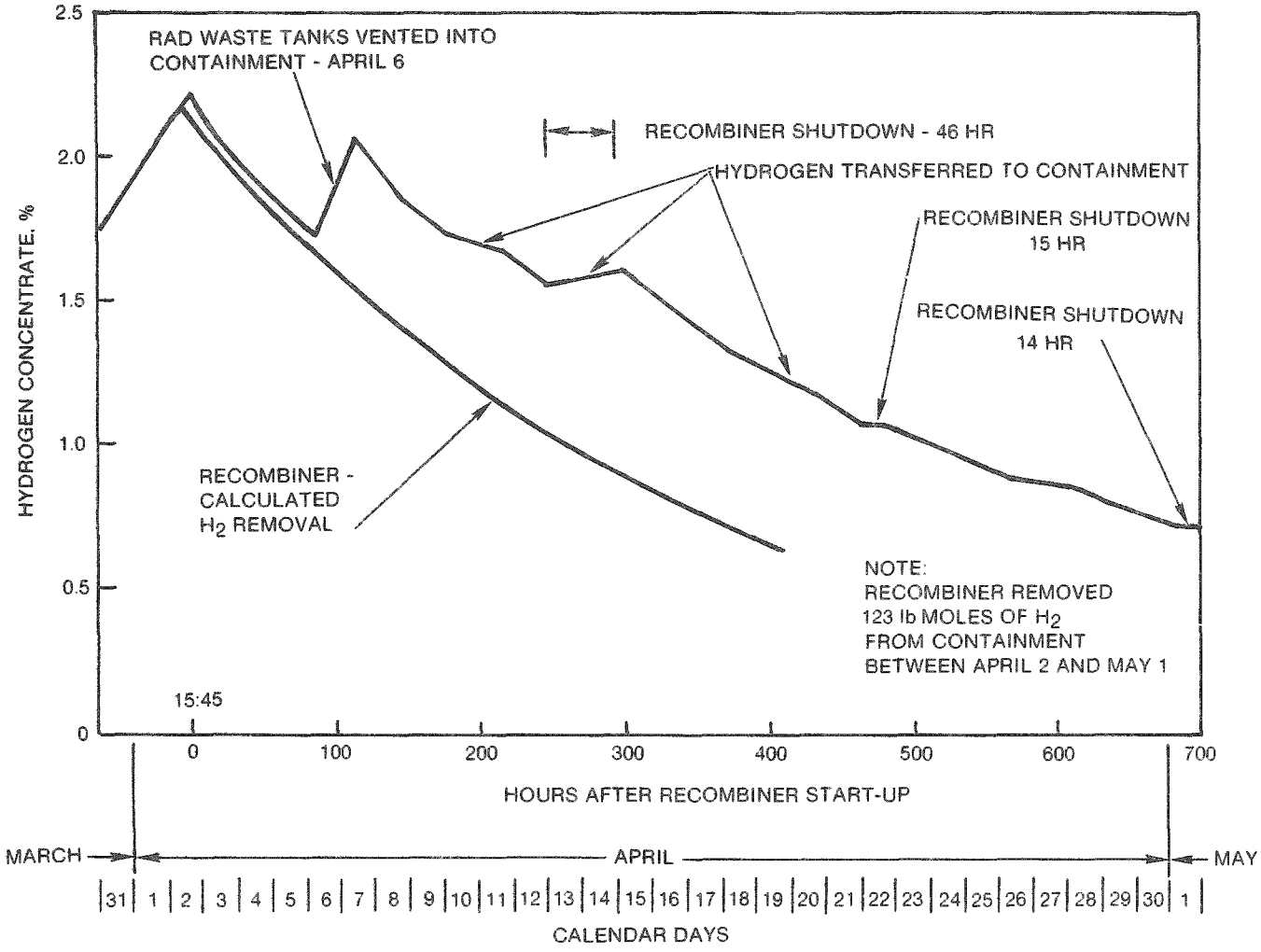

FIGURE 6-1. TMI Unit 2 Hydrogen Recombiner Operation.

TABLE 6-1. Containment Hydrogen Balance.

Time	Hydrogen added		Hydrogen removed		Hydrogen inventory	
	Dry (%)	kg	Dry (%)	kg	Dry (%)	kg
03/28/79						
13:50	8.2	370			8.2	370
13:52			7.1	319[b]	1.1	51
15:00	0.6	24[a]			1.7	75
04/01/79	0.5	21[a]			2.2	96
05/01/79	1.1	44[a,c]	2.6	112[d]	0.7	28
07/80		—	0.7	28[e]		0
Total		459		459		

[a]From RCS.

[b]Hydrogen burn.

[c]From waste gas decay tanks and radiolysis.

[d]Rockwell International Hydrogen Recombiner.

[e]Vented to atmosphere.

7.0 ACKNOWLEDGMENTS

The writers acknowledge the contributions of those who provided data, ideas, advice, and technical assistance in the preparation of this report. In particular, appreciation is expressed to the following people for their valuable effort:

- J. E. Flaherty, Energy Incorporated, and K. L. Imhof, GPU Nuclear, who provided much data in response to our many requests for data over a 3-yr period

- G. Eidam, D. Reeder, and N. Pace of EG&G Idaho, Inc. who provided photographs of burn damage and performed steady-state heat transfer calculations to check progressive dynamic calculations predicting gas-cooler outlet temperatures during and shortly after the hydrogen burn

- R. S. Gagliardo, P. K. De, S. Chou, and H. Young of Burns & Roe who researched and provided valuable details about the HVAC system, temperature and pressure instrumentation, and circuitry descriptions

- M. Smith of Rockwell Hanford Operations and M. O'Rell of Kaiser Graphics for their support in the preparation of figures, tables and editing of the report.

- Comments from the following U.S. Department of Energy (DOE)-selected peer review group: N. Alvares, Lawrence Livermore; J. Cummings, Sandia; M. Hertzberg, U.S. Bureau of Mines; J. Jacoby, EG&G; E. Marram, Geo-centers; H. Ring, DuPont; F. Stetson, NUS; H. Tamm, AECL-WNRE, Canada; F. Tooper, K. Tricket and B. Washburn, DOE; K. Parczewski, U.S. NRC; R. Zalush, Factory Mutual.

8.0 REFERENCES

1. L. W. Carlson, R. M. Knight, and J. O. Henrie, Flame and Detonation Initiation and Propagation in Various Hydrogen-Air Mixtures, With and Without Water Spray, AI-73-29, Rockwell International, Canoga Park, California (May 1973).

2. R. O. Wooten et al., Analysis of the Three Mile Island Accident and Alternative Sequences, NUREG/CR-1219, Battelle Columbus, Columbus, Ohio (January 1980).

3. R. K. Cole, Generation of Hydrogen During the First Three Hours of the Three Mile Island Accident, NUREG/CR-0913, Sandia National Laboratories, Albuquerque, New Mexico (July 1979).

4. Electric Power Research Institute, Supplement to Analysis of Three Mile Island-Unit 2 Accident, NSAC-1, Palo Alto, California (October 1979).

5. G. R. Bloom et al., Hydrogen Mixing and Distribution in Containment Atmospheres, Electric Power Research Institute, Palo Alto, California (in preparation).

6. G. R. Eidam and J. T. Haran, Color Photographs of the Three Mile Island Unit 2 Reactor Containment Building: Volume 1 - Entries 1, 2, 4, 5, 6, GEND-006, EG&G Idaho, Inc., Idaho Falls, Idaho (October 1981).

7. W. H. McAdams, Heat Transmission, 3rd Edition, pp. 85, McGraw-Hill Book Company, New York (1954).

APPENDIX

CHARACTERISTICS OF A LARGE "CONSTANT VOLUME" HYDROGEN BURN

In containment, a burn is considered to occur on a "constant volume" basis. However, if the burn occurs over a relatively long time (that is, many seconds), the burning of any single unit volume (i.e., 1 L or 1 ft^3) occurs very rapidly and burns more on a constant pressure basis. Constant pressure burning is cooler than constant volume burning because of the "expansion-cooling" which takes place during the constant pressure burn. In a closed system the energy difference between constant volume and constant pressure burning of a small volume of the gas goes into a slight compression heating of all of the remaining (burned and unburned) volume. Assuming no heat loss during the Three Mile Island (TMI-2) hydrogen burn, the initial unit volume, the middle unit volume, and the last unit volume to burn would have had the characteristics shown in Table A-1.

The theoretical, constant volume, adiabatic end-of-burn temperature is 760°C (1400°F). This temperature and the theoretical end-of-burn temperatures shown in Table A-1 are higher than the actual temperatures were since heat was lost to walls and equipment during the burn. This was particularly true of the first unit volume to burn, since it had time (~12 seconds) to lose heat from its initial 566°C (1050°F) temperatures, as the burn progressed and as compression heating occurred. The last unit volume to burn cooled at a much slower rate during the burning period since its temperature just before the end of the burn had heated (by compression) to only 168°C (335°F). Therefore the theoretical, adiabatic, temperature [860°C (1257°F)] of the last unit volume to burn is probably only slightly higher than the actual temperature. If preheating by radiant heat transfer is significant, the afterburn temperature of the last unit volume to burn could actually be higher than the 860°C calculated. The <u>average</u> containment gas temperature at the end of the burn calculated on the basis of measured pressure rise is 660°C (1200°F).

TABLE A-1. Characteristics of the First, Middle, and Last Unit Volumes to Burn, Assuming No Heat Lost During Burn.

Characteristic	First unit volume	Middle unit volume	Last unit volume
Pressure, KPa (psia)	100 (15)	200 (30)	300 (45)
Volume occupied after compression of original volume	1	0.5	0.333
Initial temperature, °C (°F)	53 (128)	53 (128)	53 (128)
Temperature just prior to burn resulting from compression heating, °C (°F)(1)	53 (128)	122 (252)	168 (335)
Temperature rise resulting from burn, °C (°F)(2)	512 (922)	512 (922)	512 (922)
Temperature immediately after burning the specific unit volume, °C (°F)	566 (1050)	634 (1174)	680 (1257)
Temperature at end of burn, after postburn compression heating, assuming no heat loss during burn, °C (°F)(3)	862 (1583)	742 (1367)	680 (1257)

(1) $\frac{T2}{T1} = \left(\frac{P2}{P1}\right)^{\frac{K-1}{K}}$

$\frac{T2}{T1} = 1.118$ for $\frac{P2}{P1} = 1.5$; 1.21 for $\frac{P2}{P1} = 2$; 1.353 for $= \frac{P2}{P1} = 3$

$K = \frac{C_p}{C_v} = 1.38$ for the wet, preburn containment gas

(2) $(1400°F - 128°F)/1.38 = 922°F = 512°C$

(3) $T2 = [(1050 + 460)]1.353 - 460 = 1583°F = 862°C$

$T2 = [(1174 + 460)]1.118 - 460 = 1367°F = 742°C$